From the Division of Medical Imaging and Technology
Department of Clinical Science, Intervention and Technology
Karolinska Institutet, Stockholm, Sweden

OPTIMIZED MRI METHODS FOR SIMPLIFIED ONCOLOGICAL IMAGING IN PANCREAS AND LIVER

Nikolaos Kartalis

Karolinska Institutet

Stockholm 2012

Published by Karolinska Institutet. Printed by Universitetsservice US-AB.

ISBN 978-91-7457-731-0

In the memory of my father Georgios

ABSTRACT

Recent technological advances within the fields of Abdominal Imaging have revolutionised oncological imaging. In the investigation of the solid organs in the upper abdomen, extensive examinations are used in order to obtain accurate information. To improve the early detection of –still curable– pathological changes, novel methods that are faster, easier and still as highly accurate as the ones currently used, are warranted; in that way, the needs for higher efficiency in the modern multidisciplinary environment can be met in a cost-effective manner.

The overall purpose of this thesis was to develop and optimise MRI methods for the simplified oncological imaging evaluation of two important patient groups:

a. those with pancreatic cancer, by applying diffusion-weighted (DW) MRI (studies I and II), and
b. those with colorectal cancer liver metastases (CRLM), by using a novel, manganese-based, orally administered MRI contrast agent (CMC-001) (studies III and IV).

In **study I**, the accuracy of DW MRI was evaluated and compared with a conventional comprehensive MRI (MRI-c) protocol in 36 patients with pancreatic lesions (12 malignant and 24 benign) and 39 without lesions. The results showed that DW MRI has an accuracy that is similarly high to that of MRI-c for the detection of pancreatic cancer.

In **study II**, three different DW MRI techniques (respiratory-triggered, free-breathing, and breath-hold) were compared regarding image quality, signal intensity and ADC measurement in 15 patients with proven pancreatic cancer. The results showed superiority of the respiratory-triggered technique in both analyses for demonstrating pancreatic cancer.

In **study III**, the sensitivity of MRI to detect CRLM after ingestion of a full-dose of CMC-001 was compared with that of a comprehensive intravenous gadobenate dimeglumine protocol as well as their safety profile and patient acceptability were compared in 20 patients suspected of having 1-6 such lesions. The results showed that CMC-001 and the intravenous gadobenate dimeglumine had similar sensitivities; no safety issues were raised for neither contrast agent but CMC-001 had higher rates of gastrointestinal adverse events.

In **study IV**, the efficacy of three different doses of the contrast agent CMC-001 (corresponding to ½, ¼ and ⅛ of the full dose) as well as its safety profile and patient acceptability were evaluated in 32 healthy volunteers. The results showed that ½ dose of CMC-001 had higher efficiency and still acceptable adverse drug reactions/adverse events.

In conclusion of studies I and II, DW MRI is as sensitive as the comprehensive MRI protocol in detecting pancreatic cancer and for that, the respiratory-triggering seems the optimal technique. In conclusion of studies III and IV, the sensitivity of the full dose of oral CMC-001 is as high as the intravenous gadobenate dimeglumine protocol but half-dose of this agent should be preferred due to higher patient acceptability.

LIST OF PUBLICATIONS

I. **Diffusion-weighted magnetic resonance imaging of pancreas tumours**
Kartalis N, Lindholm TL, Aspelin P, Permert J, Albiin N
Eur Radiol. 2009 Aug;19(8):1981-90.
Epub 2009 Mar 24. PubMed PMID: 19308414.

II. **Optimising diffusion-weighted MR imaging in demonstrating pancreas cancer: a comparison of respiratory-triggered, free-breathing and breath-hold techniques**
Kartalis N, Loizou L, Edsborg N, Segersvärd R, Albiin N
Accepted in March 2012 for publication in European Radiology.
DOI: 10.1007/s00330-012-2468-3

III. **MRI of colorectal cancer liver metastases: comparison of orally administered manganese with intravenously administered gadobenate dimeglumine**
Brismar TB, Kartalis N, Kylander C, Albiin N
Eur Radiol. 2012 Mar;22(3):633-41.
Epub 2011 Sep 28. PubMed PMID: 21953376.

IV. **Manganese chloride tetrahydrate (CMC-001) enhanced liver MRI: Evaluation of efficacy and safety in healthy volunteers**
Albiin N, Kartalis N, Bergquist A, Sadigh B, Brismar TB
MAGMA. 2012 Mar 8.
[Epub ahead of print] PubMed PMID: 22399275.

TABLE OF CONTENTS

LIST OF ABBREVIATIONS

3D	Three-dimensional
ADC	Apparent diffusion coefficient
ADR	Adverse drug reaction
AE	Adverse event
ANOVA	Analysis of variance
BH	Breath-hold
CEUS	Contrast-enhanced ultrasound
CRLM	Colorectal cancer liver metastases
CV	Coefficient of variation
DW	Diffusion-weighting
DWI	Diffusion-weighted imaging
ECG	Electrocardiogram
EPI	Echo-planar imaging
EUS	Endoscopic ultrasound
FB	Free-breathing
FNH	Focal nodular hyperplasia
Gd-BOPTA	Gadolinium benzyloxypropionictetro-acetate, or gadobenate dimeglumine
GFR	Glomerular filtration rate
HASTE	Half-Fourier acquisition single-shot turbo spin echo
HCC	Hepatocellular carcinoma
IVIM	Intra voxel incoherent motion
IU	International unit (s)
LOAEL	Lowest observed adverse effect level
MDCT	Multi-detector computed tomography
$MnCl_2$	Manganese chloride
MRI	Magnetic resonance imaging
MRI-c	Comprehensive magnetic resonance imaging
NA	Nils Albiin
NE	Nick Edsborg
NEX	Number of excitation (s)
NK	Nikolaos Kartalis

NPV	Negative predictive value
NSF	Nephrogenic systemic fibrosis
PACE	Prospective acquisition correction
PACS	Picture archiving and communication system
PDAC	Pancreatic ductal adenocarcinoma
PET-CT	Positron emitting tomography-computed tomography
PPV	Positive predictive value
RFA	Radiofrequency ablation
ROI	Region of interest
RT	Respiratory-triggering
SD	Standard deviation
SE	Spin-echo
SI	Signal intensity
SNR	Signal-to-noise ratio
SS	Single-shot
STIR	Short tau (t) inversion recovery
US	Ultrasound
T	Tesla
T1	Longitudinal relaxation time
T2	Transversal relaxation time
TB	Torkel Brismar
TE	Echo-time
VIBE	Volumetric interpolated breath-hold examination
WL	Window level
WW	Window width
Z-GFAAS	Graphite furnace atomic absorption spectrometry with Zeeman correction

1 INTRODUCTION

1.1 BACKGROUND

The technological developments that have been accomplished in recent years within the fields of Abdominal Imaging have revolutionised the diagnostics of many tumour types (1,2). Innovations, such as the availability of high-standard hardware, routine clinical application of advanced software solutions and dedicated protocols, use of intravenously (IV) administered contrast agents of various properties as well as the accumulation of knowledge among radiologists, have given Diagnostic Imaging a pivotal role in patient management.
In the investigation of pathologies of the solid organs in the upper abdomen, extensive magnetic resonance imaging (MRI) and multidetector computed tomography (MDCT) examinations are used in order to obtain accurate diagnostic information; and that, mainly due to the complex physiological behaviour of the various tumour types and the inherent difficulties in imaging organs subject to bulky motion (i.e. respiration). Images are generated both before and after the administration of IV contrast agents at multiple, predefined time-points (dynamic imaging). These time-consuming protocols, especially regarding MRI, result in the acquisition of multiple image series that have to be reviewed and analysed. Compared to MRI, MDCT examinations are faster to acquire, somehow easier to assess and more widely available at the cost of exposing the patient to –potentially harmful– ionizing radiation (3). MRI does not require the use of ionizing radiation and is a highly accurate modality for the detection of pathological changes in the earlier stages of the disease. However, due to the higher cost and the lack of availability, MRI is more often reserved as a so-called "problem-solver", i.e. it is applied when other modalities previously employed did not suffice. Most of the patients having early and rather unspecific symptoms and signs are usually not referred for examination with the aforementioned expensive and extensive modalities.

Thus, in order to improve the early detection of pathological changes, which may still be subject to curative surgery, simplified methods are warranted. These methods should be fast and easy to perform and assess, while maintaining high diagnostic accuracy. In that way, Diagnostic Imaging can meet the needs for higher efficiency that is posed by a lot of the other medical specialities in the modern multidisciplinary environment and, all that, in a cost-effective manner.

The overall purpose of this thesis was to develop and optimise MRI methods for the simplified oncological imaging evaluation of two important groups:

a. patients with pancreatic cancer, by applying diffusion-weighted (DW) MRI, and
b. patients with colorectal cancer liver metastases (CRLM), by using a novel, manganese-based, orally administered MRI contrast agent (CMC-001).

1.2 PANCREATIC CANCER

Pancreatic ductal adenocarcinoma (PDAC) is a disease with poor prognosis; the overall 5-year survival is about 5 % and one major reason is late diagnosis. At the time of

diagnosis, less than 10 % of patients are candidates for the only curative treatment, surgical resection (4). In 2008, the estimated number of new pancreatic cancer cases was 277 000 worldwide. During the same period, the estimated number of pancreatic cancer-related deaths was 266 000, suggesting that the mortality rate is 96 % of the incidence rate (5). Despite the great technical advances with imaging, such as ultrasonography, MDCT and MRI, detection of pancreatic cancer at an early stage is non-satisfactory; therefore, new and more efficient methods are required (6).

1.2.1 Diffusion-weighted Magnetic Resonance Imaging

Diffusion weighted imaging (DWI) is based upon the principles of Brownian motion (random thermal diffusion) of small molecules in a tissue. By applying diffusion weighting to a sequence (a combination of pulses and strong gradients), one can measure the apparent diffusion coefficient (ADC) in a given tissue and, thus, quantify the combined effects of capillary perfusion and water diffusion. The use of DWI as a diagnostic tool in neoplastic diseases is based on the principle that, in malignant lesions, cells have a larger volume and are more closely aligned to each other. This hypercellularity diminishes the extracellular space leading to restriction of the free movement of water particles resulting in a depressed ADC and hyperintensity (bright appearance) on DW images. In contrast, benign lesions (such as cysts, hemangiomas) are characterized by expansion of the extracellular space and not by hypercellular populations, which in turn eases the diffusion of water molecules which is displayed as high ADC and hypointensity (dark appearance) on DW images.

DWI has been used for diseases of the central nervous system for two decades (7,8) – being a particularly important tool in the diagnosis of ischemic stroke– and the musculoskeletal system for one decade (9,10). During recent years, DWI of diseases of the lower abdomen, e.g. prostate (11), urinary bladder (12), uterus (13) and rectum (14) has presented promising results. DWI of the upper abdomen has been a technical challenge due to respiration, bowel peristalsis, blood flow and long acquisition times. Technological advancements in the application of DWI, such as the use of high performance gradients, echo-planar imaging (EPI) and, more importantly, the implementation of parallel imaging have made DWI of the upper abdomen a feasible option. Valuable information can be obtained about diffuse diseases of the liver and pancreas, both qualitatively and quantitatively (the latter by measuring ADC) (15-21). In oncological imaging in particular, DWI has gained a role in the detection of malignant disease (22-26) as well as in the prediction and monitoring of treatment effects (27-30).

The DWI technique most often applied in the upper abdomen is single-shot spin-echo echo-planar imaging (SS SE EPI) incorporating parallel imaging. Image acquisition can be performed during either breath-hold (BH) or non-breath-hold modes, such as respiratory-triggered (RT) or free-breathing (FB) techniques. Non-breath-hold techniques allow for multiple averaging providing higher signal-to-noise ratio (SNR) and thinner slices than breath-hold but at the expense of longer examination time. RT substantially prolongs the examination time compared to the FB approach. However, in the latter, anatomical details are less clearly defined and the ADC quantification is

probably less precise because of volume averaging. The advantage of the BH approach is the shorter examination time and fewer respiratory-related motion artefacts, albeit at the expense of the lower SNR and spatial resolution acquired as well as the limited b-values obtained (31).

1.3 COLORECTAL CANCER LIVER METASTASES

The liver is the most common site of metastases from the gastrointestinal tract, including pancreatic, gastric, small bowel, and colorectal cancers (CRC). In 2008, the estimated number of new CRC cases was 1 233 000 worldwide. During the same period, the estimated number CRC-related deaths was 608 000 (the mortality rate being 49 % of the incidence rate) (5). At the time of diagnosis, 15-20% of patients have distant metastases and the site most commonly involved is the liver (32). During the course of the primary disease, up to 50% of patients will develop liver metastases (CRLM) (33,34). If left untreated or with only palliative chemotherapy, the 5-year survival does not exceed 1 % (35,36). However, by applying improved surgical techniques and new chemotherapy regimes, the 5-year survival can reach 60% (37,38). More than half of the patients treated with curative intent surgery (resection with/without radiofrequency ablation [RFA]), develop recurrence within two years (39).

1.3.1 Manganese chloride tetrahydrate (CMC-001)

In surveillance for CRLM, the primary imaging technique is multidetector computed tomography (MDCT) (40-42). Contrast-enhanced ultrasound (CEUS) is also reported to perform well (43). However, MRI due to its superior diagnostic sensitivity and specificity when evaluating liver lesions plays a major role (44-46). To improve the detection and characterization of lesions, a number of intravenous MRI contrast agents have been developed. Among these, two of the T1-shortening contrast agents have liver-specific characteristics: gadoxetic acid (Primovist) and gadobenate dimeglumine (MultiHance). These contrast agents have to be administered intravenously and contain gadolinium, which increases the risk of nephrogenic systemic fibrosis (NSF) in patients with low glomerular filtration rate (GFR) (47).
A liver-specific contrast medium that is not administered intravenously and which does not contain gadolinium would be of great value for evaluating patients at high risk of liver metastases. A novel manganese-based contrast agent, CMC-001, has been developed for oral administration. The active substance is manganese chloride ($MnCl_2$) tetrahydrate and is combined with alanine and vitamin D_3 serving as promoters for bowel wall absorption. Recently, $MnCl_2$ has also been combined with ascorbic acid for promoting absorption from the bowel wall (48). After ingestion, manganese is absorbed by the small bowel and transported via the portal circulation to the liver. Manganese is then taken up by functioning hepatocytes and secreted into the bile duct system. In MRI, this will cause an increase in signal intensity (SI), both of the liver parenchyma and of the bile duct system (on T1-weighted sequences, optimally between 2 to 6 hours

after ingestion) (49). Metastases and non-functioning hepatocytes do not take up manganese, and thus have low SI on T1-weighted sequences. Furthermore, up to 95% clears from the liver at first-pass. Thus, only minimal amounts of manganese reach the systemic circulation, substantially reducing the risk of adverse events (AEs) correlated with the intravenous administration of manganese (50,51). This, in combination with the convenience of self-administration of the contrast agent on an outpatient basis, 2-6 hours prior to imaging, makes the orally administered CMC-001 an interesting alternative for imaging of liver metastases.

2 AIMS OF THE THESIS

The overall purpose of this thesis was to develop and optimise MRI methods for the simplified oncological imaging evaluation of the two, previously described, important patient groups: those with pancreatic cancer as well as those with colorectal cancer liver metastases.

For that purpose, four studies were designed and performed, with specific aims as follows:

Study I
a) To determine sensitivity, specificity, accuracy, positive and negative predictive value (PPV and NPV, respectively) of DWI in detection of pancreatic cancer in patients investigated with MRI for suspected upper abdominal disease (liver, biliary tree, pancreas and kidneys/suprarenal glands),
b) To compare (in the same patient group) the results of DWI with a comprehensive MRI (MRI-c) examination protocol, which conventionally does not include DWI, and
c) To quantitatively analyse ADC values and investigate if malignant lesions can be differentiated from benign on the basis of these values.

Study II
To compare –in patients with pancreatic cancer– respiratory-triggered, free-breathing and breath-hold DWI techniques in terms of a) subjective image quality and b) signal intensity (SI) characteristics and ADC measurements at 1.5 Tesla.

Study III
a) To evaluate whether the sensitivity of a full dose (i.e. 1.6 g manganese) of the new contrast medium to detect colorectal cancer liver metastases (CRLM) was comparable to that of a comprehensive gadobenate dimeglumine protocol, and
b) To assess the safety profile and patient acceptability of the full dose of CMC-001.

Study IV
a) To evaluate –in healthy volunteers– the efficacy of three different doses of the contrast agent CMC-001, corresponding to ½, ¼ and ⅛ of the full dose (i.e. 0.8 g, 0.4 g and 0.2 g manganese, respectively), and
b) To assess the safety profile and patient acceptability of these three different doses of CMC-001.

3 MATERIALS AND METHODS

All four studies were approved by the ethical committee at Karolinska Institutet, in Stockholm, Sweden.

3.1 PATIENTS

Study I: During the period October 2006 – June 2007, 305 patients referred to our Radiological Department at Karolinska University Hospital, Huddinge –for an MRI examination of the upper abdomen (liver, bile ducts, pancreas, spleen and kidneys/suprarenal glands)– were examined in a prospective and consecutive manner with the use of our standard comprehensive upper abdomen protocol and additional DWI. Totally 75 patients fulfilled the inclusion criteria: (i) having a good overall diagnostic quality comprehensive MRI examination and additional DWI, and (ii) either histopathological proof or clinical and cross-sectional imaging follow-up ≥6 months (230 patients were excluded: *n*=24 had other MRI protocol not including DWI, *n*=14 had examination of suboptimal quality and *n*=192 had either no surgery or cross-sectional imaging follow-up <6 months). Eighteen of these underwent pancreatic surgery or had diagnostic biopsy (male/female: 10/8, mean age: 63 years) and 57 had a cross-sectional imaging follow-up of at least 6 months that was of good overall diagnostic quality (male/female, 28/29, mean age: 47 years). Of the 75 analysed patients, 39 had no lesion found, 12 had a malignant lesion (mean lesion size: 3.7 cm and standard deviation/SD: 1.9 cm) and 24 a benign lesion (mean lesion size: 2.3 cm and SD: 2.3). The prevalence of pancreatic cancer in the study population was 16 %.

Study II: During the period May 2010 – May 2011, 16 consecutive patients fulfilled the inclusion criteria: (i) high suspicion of PDAC, based on previous clinical history and imaging findings, and undergoing surgical treatment with curative intention, (ii) no history of previous chemo- or radiation therapy, and (iii) no contraindication for MR examination. They were enrolled on a preliminary basis after providing their informed consent. Of these patients, one was excluded because the post-operative histopathological findings showed a tumour other than PDAC (gallbladder carcinoma). Hence, the study population comprised 15 patients (male/female: 8/7, mean age: 64 years) with histopathologically verified PDAC. Mean lesion size was 3.2 cm (SD: 0.6 cm) and 12 were located in the head, 1 in the body and 2 in the tail of the pancreas.

Study III: During the period November 2005 – September 2007, 20 patients (male/female: 10/10, mean age: 64 years) were recruited prospectively and consecutively. All patients had been referred to the multidisciplinary team at our hospital for evaluation of 1 – 6 suspected CRLMs before partial liver resection. The suspected metastases had been observed at contrast-enhanced MDCT in 17 patients and at MRI in 3 patients. In addition, nine of the patients had undergone a contrast-enhanced transabdominal ultrasound. At the final analysis (histopathology, additional imaging or follow-up) one or more metastases were found in 16 of the 20 patients; in 4 patients there were no metastases. In total, 44 metastases were identified (mean size: 19.5 mm, SD: 15.6, size range: 3 – 73 mm). Metastases were verified at histopathology after surgery (*n*=25), at combined evaluation of contrast-enhanced ultrasound and

gadobenate dimeglumine-enhanced MRI by a consensus committee consisting of radiologists and surgeons at the multidisciplinary conference (*n*=7), contrast-enhanced ultrasound performed at least 3 months later (*n*=8), intra-operative contrast-enhanced ultrasound (*n*=3) or contrast-enhanced MDCT 3 months later (*n*=1). The absence of metastatic lesion in four patients was confirmed by histopathology in two, by combined evaluation of contrast-enhanced ultrasound and gadobenate dimeglumine-enhanced MRI in one patient and, finally, by MDCT examination performed three months later in one patient. In these four patients, the suspected metastasis had been observed at MDCT in three patients and at gadoxetate disodium-enhanced MRI in one.

Study IV: Between February and May 2010, 32 healthy volunteers (males/females: 18/14, mean age 24.3 years) fulfilled the inclusion criteria and were preliminarily randomized (for a more thorough description of inclusion and exclusion criteria, the reader is referred to the published study IV presented at the end of the thesis). Two of them were excluded from the study: one withdrew the approval for personal reasons and one was excluded due to an incidentally found focal nodular hyperplasia (FNH). Both subjects were excluded after administration of one dose level of CMC-001, allowing their inclusion in the safety analysis. In total, 30 volunteers completed the study.

3.2 METHODS

3.2.1 MRI protocol

The MRI examinations for all four studies were performed using a commercially available 1.5 T MRI system (Magnetom Avanto, Siemens Medical Solutions, Erlangen, Germany) with body and spine matrix coil combination. For a thorough description of the technical details of the imaging parameters, the reader is referred to the respective published articles presented at the end of this thesis.

Study I: The comprehensive MRI upper abdomen clinical protocol (MRI-c), serving as the standard examination in our daily practice was used and included standard T1- and T2-weighted sequences and 3D T1-weighted VIBE (volumetric interpolated breath hold examination) for dynamic imaging. A power injector was used for the intravenous administration of the contrast agent gadobenate dimeglumine, or Gd-BOPTA, (MultiHance, Bracco, Milan, Italy; 0.1 mmol/kg body weight at an injection rate of 2 ml/sec) and the Care Bolus technique to ensure correct timing of the late arterial/parenchymal (when the pulmonary arteries were well filled with contrast the patient was commanded to hold his/her breath; thereafter, the acquisition of the VIBE sequence was started) and venous phase (acquisition was started 50 sec after start of arterial phase). Delayed venous phase was acquired 5 minutes after start of injection of contrast, as well as a supplementary liver-specific phase 2 hours later (and that for detection of liver metastases, should they be present). DWI was not a part of the MRI-c analysis.

The DWI sequence (b-values 0 and 500 s/mm^2) was acquired under free breathing using three acquisitions for averaging (number of excitations-NEX 3), STIR fat saturation and with the diffusion gradients applied in three orthogonal directions. An inter-slice gap of 1.5 mm was used. ADC maps were automatically generated on the MRI system's console.

Study II: All patients underwent SS SE EPI DWI of the pancreas with five b-values (0, 50, 300, 600 and 1,000 s/mm^2) with all three breathing techniques: RT, FB, and BH. For the RT technique, the prospective acquisition correction (PACE) technique was used. For the BH technique, DW images at each b-value were obtained on a single breath-hold at end inspiration. Coronal T2-weighted half-Fourier acquisition single-shot turbo spin-echo (T2-HASTE) images at both end inspiration and end expiration were obtained before the DWI techniques for optimal slice positioning. ADC maps for the RT and FB techniques were generated automatically on the MRI system's console (ADC_{RT} and ADC_{FB}, respectively) and generated manually for the BH technique (ADC_{BH}) with a dedicated workstation (Leonardo, Siemens Healthcare, Erlangen, Germany) by fitting all the b-values in the formula: $S/S_0 = \exp(-b \bullet ADC)$, where S_0 corresponds to the signal without and S to the signal with diffusion weighting. No intravenous contrast agent was used.

Study III: Two MRI examinations were performed on each patient at an interval of one week; orally administered manganese-based contrast medium CMC-001 (CMC Contrast, Lyngby, Denmark) or intravenously administered gadobenate dimeglumine (MultiHance, Bracco, Milan, Italy) was used in random order, based on sealed envelopes.

The patients arrived at the MR unit early in the morning after one night of fasting. Imaging was performed before administration of contrast medium and either 3 hours after oral ingestion of CMC-001 or after intravenous gadobenate dimeglumine using a 5-phase imaging protocol (unenhanced, arterioportal, portal venous, 5 min and 2 hours), serving as our standard protocol in daily practice. The dose of CMC-001 was equivalent to 1.6 g $MnCl_2$ and was dissolved in 200-400 mL of water. The dose of gadobenate dimeglumine was 0.1mmol/kg.

For T1-weighted imaging, axial breath-hold 3D T1-weighted images (VIBE) were obtained and for T2-weighted imaging, axial T2-HASTE images were used. Total MR examination time for CMC-001 session was about 10 minutes each for pre- and post-contrast imaging. At the gadobenate dimeglumine session, the total MR examination time was 60+10 minutes.

In all cases of contrast-enhanced ultrasound, the microbubble-containing contrast agent sulphur hexafluoride (SonoVue, Bracco, Milan, Italy) was injected in a single dose of 2.4 mg/ml followed by a flush of 5-10 ml isotonic saline; when needed, the injection was repeated in order to evaluate the whole liver.

For patient safety, all examinations were evaluated at the time of the examination by one of the participating radiologists (NA) and the imaging findings were discussed at the multidisciplinary conference for decision-making. After a period of at least 6 weeks all examinations were re-evaluated in consensus by the two participating radiologists (NA and TB) for the purposes of the present study. The participating radiologists were aware that all patients had been referred for surgical procedure, but did not have access to previous studies or surgical outcome.

Study IV: After an initial screening, including clinical examination (physical examination, assessment of vital signs, electrocardiogram and recording of concomitant medication) and laboratory evaluation (plasma clinical chemistry, haematology and urinalysis), each participant underwent a liver MRI on 3 occasions: on visits 1, 2, and 3. Liver MRIs were performed both before and after administration of one of the three different dose levels of CMC-001 (CMC Contrast AB, Lyngby, Denmark). Visit 1 was scheduled no more than 21 days after initial screening. Visits 1, 2, and 3 were separated by wash-out periods of at least 6 days (i.e. 6 x 24 hours). By the completion of the study, each volunteer had received one dose from each dose level in a double-blind and random fashion. The dose levels used were:
i) 0.8 gram Mn_2Cl tetrahydrate, 0.5 gram alanine and 800 (IU) vitamin D_3 corresponding to ½ of the full dose,
ii) 0.4 gram Mn_2Cl tetrahydrate, 0.25 gram alanine and 400 (IU) vitamin D_3 corresponding to ¼, of the full dose, and
iii) 0.2 gram Mn_2Cl tetrahydrate, 0.125 gram alanine and 200 (IU) vitamin D_3 corresponding to ⅛ of the full dose.
The CMC-001 sachets were dispensed in ordinary cold tap water and each dose was administered as 200 mL oral solution.

Every examination included a T1-weighted sequence for study analysis and a T2-weighted sequence (T2-HASTE) in the axial plane for characterization of incidental findings (such as cysts and haemangiomas, should they be present). The 3D T1-weighted sequence was a fat-saturated VIBE, in the axial plane at end inspiration, which was repeated once to minimize the risk of breathing-correlated artefacts.

3.2.2 Image evaluation

Study I: Entry and exclusion of patients for analysis was performed by one radiologist (NK) having full access to the medical history, imaging and the histopathological findings. After 6-8 weeks all included examinations were retrospectively analysed, in random order without access to final diagnosis, in consensus by two radiologists (NA+NK). The analysis was done using a dedicated diagnostic workstation (Leonardo, Siemens Medical Solutions, Erlangen, Germany). Apart from the diffusion-weighted series including the ADC maps, the radiologists had access to the axial T2-HASTE sequence that served as an anatomical reference.

Image analysis was performed in two parts, as follows:

Qualitative analysis: a) Direct visual assessment of the DW images for detection of lesions and the corresponding ADC maps for characterizing them as benign or malignant (the latter having high signal on DW images with a b-value of 500 s/mm² and low signal intensity on ADC map compared to the adjacent parenchyma). All results were recorded and the patients classified as having benign, malignant or no lesions at all.
b) The results of the DWI were compared to the results of the comprehensive MRI examination protocol. In the MRI-c, the criteria favouring the diagnosis of a adenocarcinoma were a relatively well demarcated lesion with decreased enhancement compared to background parenchyma in the parenchymal phase, and with a smoothly or beaded upstream dilatation of the pancreatic duct, exhibiting abrupt interruption. Imaging findings indicating a mass-forming pancreatitis were a relatively ill demarcated lesion with the pancreatic duct being upstream irregular and having a normal or smoothly stenotic calibre inside the mass ("duct penetrating" sign). In the case of neuroendocrine tumours, criteria were a lesion exhibiting high signal intensity on T2-HASTE images and intense enhancement in the parenchymal phase.
Quantitative analysis: The apparent diffusion coefficient (ADC) of lesions was attained by drawing a region of interest (ROI) in the lesions –both benign and malignant– on the corresponding ADC maps. There was an effort to have three ROIs in the lesions and three ROIs in the remaining pancreatic parenchyma both down- and upstream, trying to avoid vessels, pancreatic and common bile ducts. The average of these three values in every different part was recorded. In normal subjects, three ROIs were placed in each anatomical part of the gland (head, body, tail) and the average of each part was recorded. There was no quantitative analysis performed in patients with lesions smaller than 10 mm (n=10 patients) due to possible partial volume averaging effects.

Study II: Image analysis was performed in two parts, as follows:

Qualitative analysis: Two radiologists with full knowledge of the study objectives (NA and NE with 11 and 9 years of experience respectively in interpreting MRI examinations of the pancreas in daily practice) reviewed the examinations independently in a blinded fashion on a commercially available PACS workstation (Sectra, Linköping, Sweden). The evaluation was performed in two parts:
a) Evaluation of DW images and ADC maps of the three techniques (DW images including ADC maps of each technique were viewed all together and independently of the DW images and ADC maps of the other techniques, in random order). For DW images, the following three parameters were rated on a four-point scale: lesion detection (4 = excellent, 3 = good, 2 = fair, 1 = poor), anatomy (4 = excellent, 3 = good, 2 = fair, 1 = poor) and presence of artefacts (4 = absent, 3 = few, without interfering with analysis, 2 = many, interfering with analysis, 1 = immense). Their sum was the score of DW images (the lesion detection parameter was assigned a weighting factor of two). For ADC maps, two parameters were rated: lesion characterization by means of lesion SI compared to the adjacent parenchyma, on a three-point scale (3 = lower SI, 2 = equal SI, 1 = higher SI) and overall image quality on a four-point scale (4 = excellent, 3 = good, 2 = fair, 1 = poor). Their sum was the score of ADC maps.
A total image quality score was calculated for each technique: the sum of scores from DW images and ADC maps, and
b) Ranking of the techniques (all three viewed simultaneously) was carried out taking into consideration all the aforementioned parameters (i.e. lesion detection, anatomy and artefacts for DW images, and for ADC maps, lesion characterization and overall image quality) as superior (3), intermediate (2), or inferior (1). Results were recorded.
The two observers had access to a coronal T2-HASTE image.

Quantitative analysis: Once the qualitative analysis had been completed, one of the radiologists who had participated in the qualitative analysis (NA) along with another radiologist (NK), with 4 years' experience in abdominal radiology, performed the quantitative analysis in consensus, blinded to the final diagnosis. The analysis was done on a commercially available PACS workstation (Sectra, Linköping, Sweden). All images of all techniques were viewed simultaneously for the quantitative analysis, which was performed in two parts:
a) Evaluation of DW images. For signal intensity characteristics, the lesion SI was measured, and the lesion SNR was calculated.
For the lesion SI measurement, a circular region of interest (ROI) was drawn onto DW images of b-values 50, 300, 600 and 1,000 s/mm^2, encompassing as much of the lesion as possible while avoiding areas of large vessels, pancreatic and common bile ducts as well as artefacts. Two or three non-overlapping ROIs were drawn on the slice(s) where the lesion was at its largest, and the average of these was recorded.
For the lesion SNR, the formula used was:

$$\mathbf{SNR_{Lesion} = SI_{Lesion}/SD_{noise}}, \text{ where } SD_{noise} \text{ is the standard deviation of noise.}$$

Because of spatially varying image noise at the application of parallel imaging, the literature suggests performing noise measurements in a homogenous region in close proximity to the signal intensity measurement site (52). Therefore, for noise measurements, we chose homogenous areas of fat in the posterior peri-pancreatic

space. Depending on the number of ROIs obtained for the corresponding lesion, two or three measurements were performed and their average was recorded, and

b) Evaluation of ADC maps. For ADC measurements, ROIs were drawn onto all ADC maps (i.e. ADC_{RT}, ADC_{FB} and ADC_{BH}) in a similar way as described above for lesion SI. The average of two or three values was recorded. For calculating the coefficient of variation (CV) of ADC, the standard deviation (SD) of the ROIs used for ADC measurement were used in the following formula:

CV= SD of ADC/mean ADC x 100 %

Study III: Image analysis was performed in two parts, as follows:

Lesion detection analysis: The non-enhanced series were first evaluated, then the corresponding contrast-enhanced series. In 10 patients, the CMC-001-enhanced examination was evaluated first; in the other 10, the comprehensive gadobenate dimeglumine examination was evaluated first. Irrespectively of order, the CMC-001 and the dimeglumine session were evaluated with an interval of at least one week. When evaluating CMC-enhanced images, both T1-weighted and T2-HASTE images were used. Criteria for the diagnosis of metastasis were low signal intensity at T1-weighted images and slightly high signal intensity at T2-HASTE images. Criteria for classifying a lesion as non-metastatic (i.e. haemangioma or/and cyst) were low signal intensity at T1-weighted images and markedly high signal intensity at T2-HASTE images. When evaluating gadobenate dimeglumine-enhanced images, the whole comprehensive protocol was used. Criteria for the diagnosis of liver metastasis were slightly hyperintense appearance in the T2-HASTE series, discrete peripheral rim contrast enhancement in the arterial and/or portal venous phases, and hypointense appearance in the liver-specific phase of the contrast enhanced series (2 hours after administration of contrast medium). Criteria for the diagnosis of haemangioma were presence of discontinuous nodular peripheral enhancement following intravenous contrast agent administration and markedly high signal intensity at T2-HASTE series. Criteria for the diagnosis of cyst were absence of enhancement following intravenous contrast agent administration and markedly high signal intensity at T2-HASTE series. The number of metastases and their greatest diameter were recorded.

Quantitative analysis: The two participating radiologists (NA and TB) performed the quantitative analysis shortly after the lesion detection analysis was completed. There were two sets of unenhanced images of the liver: one before CMC-001 and one before gadobenate dimeglumine. For the calculations of lesion signal intensity before contrast medium administration, the chronologically first of the two unenhanced series was used; for the calculations after contrast administration, only the hepatospecific phases were used (i.e. the T1-weighted image 3 hours after ingestion of CMC-001 or the T1-weighted image 2 hours after intravenous injection of gadobenate dimeglumine, respectively).
The signal intensity of the metastasis was obtained from a centrally placed circular ROI with half the diameter of the metastasis. The signal intensity of the surrounding liver was obtained from a representative region near the metastasis, in the same image, on the same anteroposterior level. The metastasis-to-liver ratio was calculated as:

Metastasis-to-liver ratio = (Liver SI-metastasis SI)/ Liver SI

Study IV: On completion of the study, all images were evaluated in consensus by two radiologists (NA and TB) experienced in abdominal imaging (10 and 6 years, respectively). The evaluation was performed on a PACS workstation (Sectra, Linköping, Sweden). At the time of image evaluation, both radiologists were blinded to the doses given. The efficacy variables were assessed by using the images derived by the T1-weighted sequence, at baseline and post-contrast. Data for assessing the efficacy variables were obtained from volunteers who completed the study (*n*=30). There were one primary and six secondary variables.

Primary variable: The primary efficacy variable was the calculation of the increase in liver-to-muscle signal intensity (SI) ratio from baseline (SI_{pre}) to post-contrast (SI_{post}). A circular region of interest (ROI) was placed in corresponding locations at the liver parenchyma and paraspinal musculature on baseline and post-contrast images avoiding degrading artefacts. The following formula was used to calculate the increase in liver-to-muscle signal intensity (SI) ratio:

$$\mathbf{SI_{post} - SI_{pre} = (Liver\ SI_{post} / Muscle\ SI_{post}) - (Liver\ SI_{pre} / Muscle\ SI_{pre}).}$$

Secondary variables:
i) Relative increase in the signal intensity of the liver from baseline to post-contrast: A circular ROI was placed in corresponding locations at the liver parenchyma on baseline and post-contrast images. The following formula was used to calculate the relative increase in liver SI:

$$\mathbf{[Liver\ SI_{post} - Liver\ SI_{pre}) / Liver\ SI_{pre}] \times 100\ \% *}$$

{* this formula was accidentally written $[(Liver\ SI_{post} - Liver\ SI_{pre}) / Liver\ SI_{post}] \times 100$ %, in the published original article}.
ii) Ranking of overall image quality of post-contrast images: Overall image quality was defined as the ability to delineate peripheral small liver vessel branches in combination with the subjectively assessed signal-to-noise ratio (SNR). The image set presenting the most satisfactory overall image quality was ranked superior, the second best intermediate, and the least satisfactory inferior. The window level was automatically optimized for each visit by pressing F1 on the workstation; thereby the mean SI of all image-generating voxels in the image was set as the window level (WL) while 4 times their standard deviation was used as the window width (WW).
iii) Overall contrast medium uptake in the liver: The window level was the same for all visits, and was the same automatic optimized level and width of the pre-contrast series (as described above). The assessment was performed subjectively and the uptake was defined in a four-point scale as excellent, good, fair or poor.
iv) Homogeneity of contrast medium uptake in the liver: The assessment was performed subjectively and the homogeneity was defined in a three-point scale as homogeneous, slightly inhomogeneous or patchy.

3.2.3 Safety analyses

Safety analysis was performed for studies III and IV.

Study III: Patients were carefully monitored for occurrence of AE (adverse events) at 1 and 2 hours after contrast medium administration and were additionally contacted by telephone at 24 and 48 hours after each product administration for a follow-up of any on-going or additional AE. AE were judged by the investigator as mild, moderate, or severe and those judged as having a reasonable causal relationship to the contrast agents qualified as adverse drug reactions (ADR). Other safety variables evaluated both before and at various time points after contrast medium administration included clinical laboratory assessments (serum clinical chemistry, haematology, serology, urinalysis), vital signs (blood pressure and heart pulse rate), electrocardiogram (ECG) and physical examination (data not shown).

Study IV: For the evaluation of safety and acceptability of CMC-001, the following variables were assessed based on data obtained from individuals who were exposed to at least one dose level of CMC-001 (i.e. the 30 individuals that completed the study and the 2 individuals that were excluded from the efficacy evaluation):
i) Adverse events. Monitoring of occurrence and follow-up of AEs was done at 1, 2 and 3 hours after contrast administration on each visit. Furthermore, after the participants left the imaging suite, they were contacted by telephone at 24 hours, 48 hours and on day 6 after contrast administration. The investigator judged all AEs as mild, moderate or severe. ADRs are those AEs that are possibly or probably related to the administration of CMC-001.
ii) Physical examination before and 3 hours after contrast administration. The physical examination included the evaluation of the volunteer's general appearance, mouth and throat, heart, lungs, abdomen and neurological system (assessed as normal or abnormal; in case of abnormal findings, these were classified as clinically significant or not).
iii) Vital signs (blood pressure and heart rate) before and at 1, 2 and 3 hours after contrast administration.
iv) Electrocardiogram (ECG) before and 3 hours after contrast administration.
v) Clinical laboratory evaluation (clinical chemistry, haematology, urinalysis) before and 3 hours after contrast administration.
vi) Manganese blood concentration, before and 3 hours after contrast administration, was determined using Graphite Furnace Atomic Absorption Spectrometry with Zeeman background correction (Z-GFAAS). The reference range is 0-330 nmol/L.

3.2.4 Statistical analyses

The statistical analyses for all studies were performed using SAS statistic software (The SAS system for Windows 9.2, SAS Institute Inc., Cary, NC, USA). A *P*-value of <0.05 was considered as significant.

Studies I and II: Multiple comparisons of continuous data were performed by analysis of variance (ANOVA). In the case of a statistically significant result in the ANOVA, statistical comparisons were made using the post-hoc test proposed by Fisher to control for multiplicity. Statistical comparisons in order to test differences between two groups were made by use of Student's t-test for uncorrelated means, after validation for normal distribution by use of the Shapiro-Wilk test. The within group analysis was made by use of pair-wise Student's t-test for correlated means. In order to evaluate hypotheses of variables in contingency tables, the chi-square test was used or, in the case of small expected frequencies, Fisher's Exact Test. In addition, descriptive statistics and graphical methods were used to characterize the data.

Study III: The calculation was based on a one-sample t-test. Non-parametric tests were assessed by McNemar's test (number of metastases after CMC-001 vs. unenhanced and after gadobenate dimeglumine vs. unenhanced). Parametric test (comparison of metastasis to liver ratio) was done by using Student's paired t-test.

Study IV: An ANOVA for the cross-over design was used to compare dose levels for the primary variable. Since the result from the carry-over test was not significant on a 5% level, a model without carry-over effects was used to make pairwise comparisons between the dose levels. Adjustment of the statistical significance level was made using the Hochberg's method. The non-parametric Wilcoxon signed-rank test was performed as a sensitivity analysis of the pairwise comparisons for the primary variable. Otherwise, the statistical analysis was performed as discussed previously in studies I and II.

4 RESULTS

Study I: The study results were as follows:

Qualitative analysis: In direct visual assessment, 11 out of 12 malignant lesions were detected and correctly characterized with DWI, while all (12 /12) with comprehensive MRI (Figure 1).

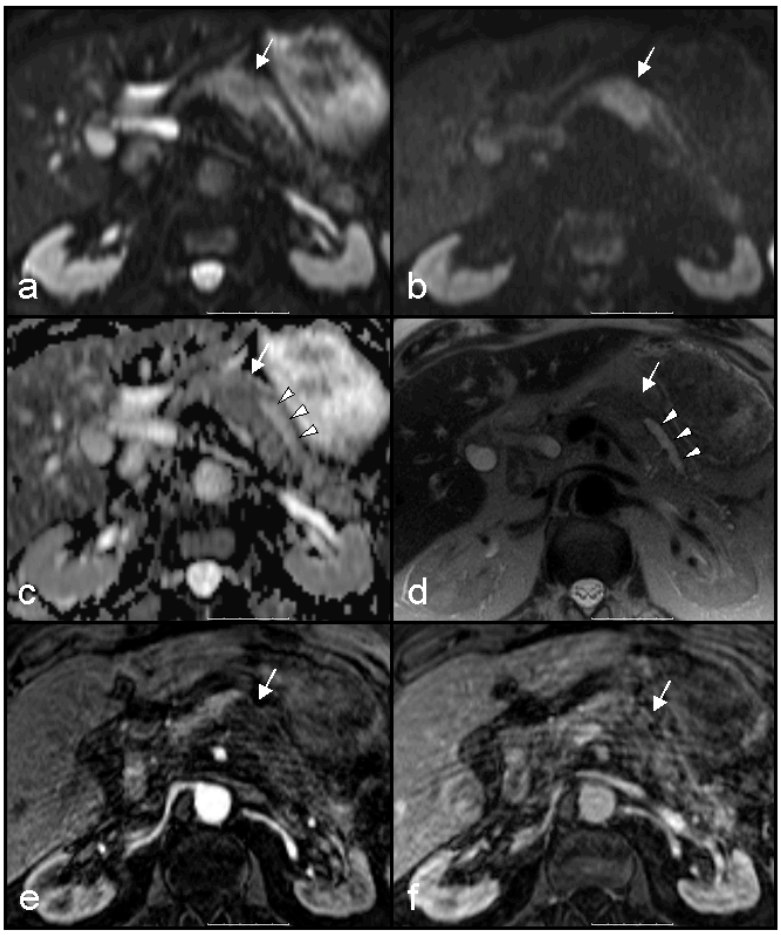

Figure 1. MR images of a patient with histopathologically proven pancreatic adenocarcinoma. The lesion (arrow) showed high signal intensity in DW images with b-values of 0 (a) and 500 (b) compared with the adjacent parenchyma and low signal intensity on corresponding ADC map (c), findings typical for malignancy. On the T2-HASTE image (d), the lesion had relatively low signal intensity and there was upstream dilatation of the pancreatic duct (arrowheads). In the parenchymal phase of the contrast-enhanced dynamic VIBE series (e), the tumour exhibited relatively well demarcated, decreased contrast enhancement that gradually increased in the venous phase (f) and was correctly characterized as malignant

Out of the 24 benign lesions, 22 were correctly characterised with both DWI and MRI-c. There were two false positive lesions with both DWI and MRI-c: one patient with a pseudocyst and one with a small lymph node (using DWI), and two patients with mass-forming pancreatitis (at MRI-c). Furthermore, there was one false negative case with DWI (neuroendocrine tumour) and none with MRI-c. The accuracy was 96 % for DWI and 97 % for MRI-c (Table 1).

Table 1. Qualitative analysis of DWI and MRI-c for pancreatic carcinoma

	Sensitivity	Specificity	Accuracy	PPV	NPV
DWI	92 %	97 %	96 %	85 %	98 %
MRI-c	100 %	97 %	97 %	86 %	100 %

Quantitative analysis: The mean ADC value of the malignant lesions was significantly lower compared to benign lesions (presented in Table 2). The ADC values of malignant and benign lesions are presented as a boxplot and scatterplot diagram in Figure 2; in this diagram there is clear overlap with four benign lesions being in the range of malignant lesions. The ADC values of the various malignant lesions are presented as a scatterplot diagram in Figure 3.

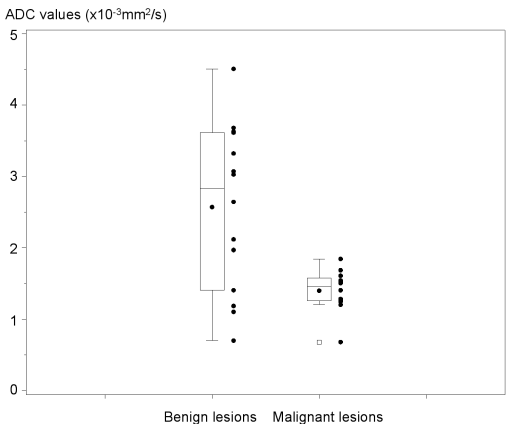

Figure 2. Boxplot and scatterplot of the ADC values of benign and malignant lesions

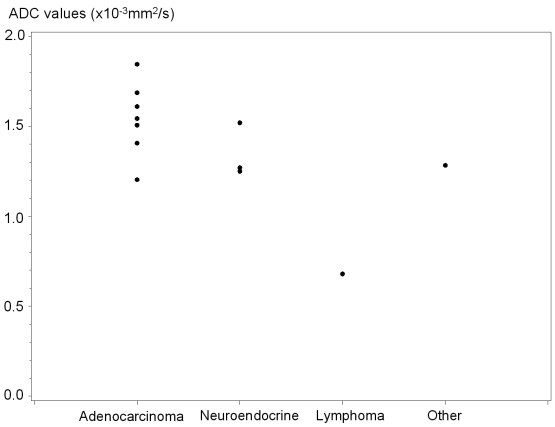

Figure 3. Scatterplot of the ADC values of the various malignant lesions

The difference between the ADC value of the lesion and the parenchyma (upstream or downstream or mean value of upstream and downstream) was significantly lower in malignant lesions compared to benign (*P*=0.0003, 0.0184 and 0.0126 respectively; the latter presented in Table 2). The ratio between the ADC value of the lesion and the parenchyma (upstream or downstream or mean value of upstream and downstream) was significantly lower in malignant lesions compared to benign (*P*=0.0004, 0.0298 and 0.0198 respectively; the latter presented in Table 2).

Table 2. Quantitative analysis of DWI for pancreatic carcinoma

	Mean ADC[1] (SD)	ADC[1] (SD) difference lesion-parenchyma[2]	ADC[1] (SD) ratio lesion/parenchyma[2]
Benign	2.57 (1.17)	1.33 (0.88)	1.87 (0.62)
Malignant	1.40 (0.30)	-0.34 (0.29)	0.82 (0.16)
P-value	0.0025	0.0126	0.0198

[1] ADC values expressed in 10^{-3} mm^2/s;

[2] mean value of upstream and downstream

In subjects with no lesions, the mean ADC value of the pancreatic head, body and tail were 1.61 (SD=0.25), 1.68 (SD=0.22) and 1.55 (SD=0.21) x 10^{-3} mm^2/s, respectively.

Study II: The study results were as follows:

Qualitative analysis:
a) The total image quality scores (average of two readers) for the RT, FB and BH techniques were 17.9, 16.5 and 17.1 respectively (Table 3 and Figure 4). The total image quality score of RT was significantly higher compared to FB and higher –but not significantly– compared to BH.

Table 3. Total image quality score as well as rating of all individual parameters (for details, please see Materials and Methods section) of respiratory-triggered (RT), free-breathing (FB) and breath-hold (BH) techniques for each reader and their average

	Detec-tion	Ana-tomy	Arte-facts	DWI score[1]	Characte-risation	Qua-lity	ADC score	Total image quality score[2]
RT								
Reader 1	3.60	3.47	2.73	13.40	2.87	3.00	5.87	19.27
Reader 2	2.93	2.87	2.87	11.60	3.00	1.93	4.93	16.53
Average	3.30	3.16	2.80	12.50	2.93	2.47	5.40	17.90[a]
FB								
Reader 1	3.20	2.80	2.53	11.73	2.80	2.60	5.40	17.13
Reader 2	2.87	2.60	2.80	11.00	3.00	1.87	4.87	15.87
Average	3.03	2.70	2.67	11.37	2.90	2.23	5.13	16.50[b]
BH								
Reader 1	3.47	3.13	2.53	12.6	2.93	2.47	5.40	18.00
Reader 2	3.13	2.73	2.80	11.8	3.00	1.40	4.40	16.20
Average	3.30	2.93	2.67	12.20	2.97	1.93	4.90	17.10[c]

[1]The parameter 'detection' was assigned a weighting factor of 2
[2]The sum of DWI and ADC score
a vs. b: significant
a vs. c and b vs. c: not significant

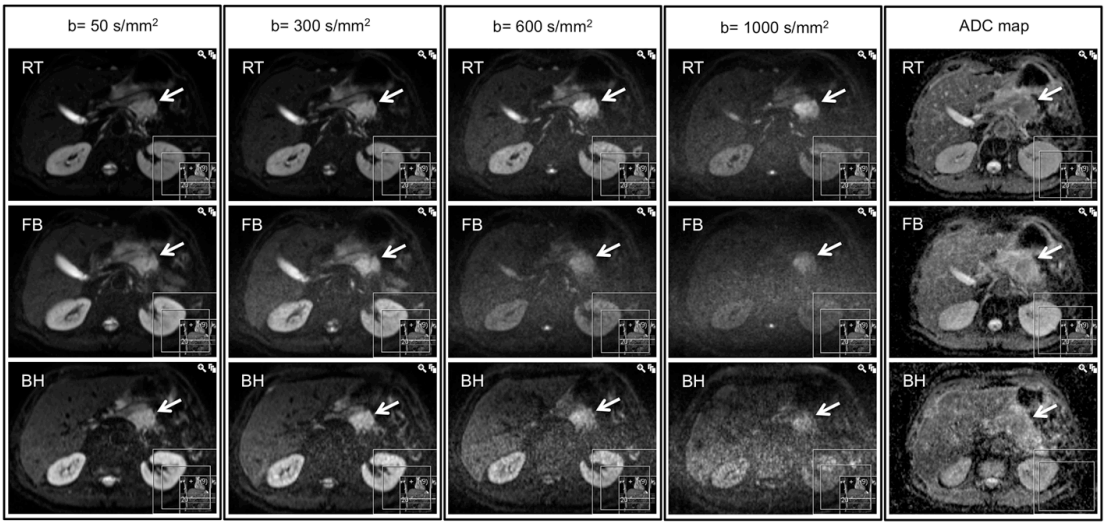

Figure 4. A typical imaging example of the total image quality score and ranking of all three breathing techniques and all b-values used in a patient with pancreatic adenocarcinoma (arrow). For this patient, the total image quality score (mean of two readers) was 19 for respiratory-triggered (RT; upper row), 16 for free-breathing (FB; middle row) and 15 for breath-hold (BH; lower row). Both readers ranked RT superior, FB intermediate and BH inferior

b) Regarding ranking of the techniques, RT was ranked significantly higher compared to both FB and BH (2.6, 1.6, and 1.8 respectively). Table 4 presents the ranking of the three techniques for each reader and their averages. A typical imaging example of ranking is presented in Figure 4.

Table 4. Ranking of RT, FB and BH sequences for each reader and their average

	RT	FB	BH
Reader 1	2.4	1.4	2.2
Reader 2	2.9	1.7	1.4
Average*	2.6	1.6	1.8

*RT vs. FB and RT vs. BH: significant
FB vs. BH: not significant

Quantitative analysis:

a) Lesion SI on all b-values was significantly higher for RT compared to FB and BH. Lesion SNR on b300 and b600 was significantly higher for RT compared to FB and BH. Lesion SNRs on b50 and b1000 for RT were higher –but not significantly– compared to FB and significantly higher compared to BH (Figure 5 and Table 5).

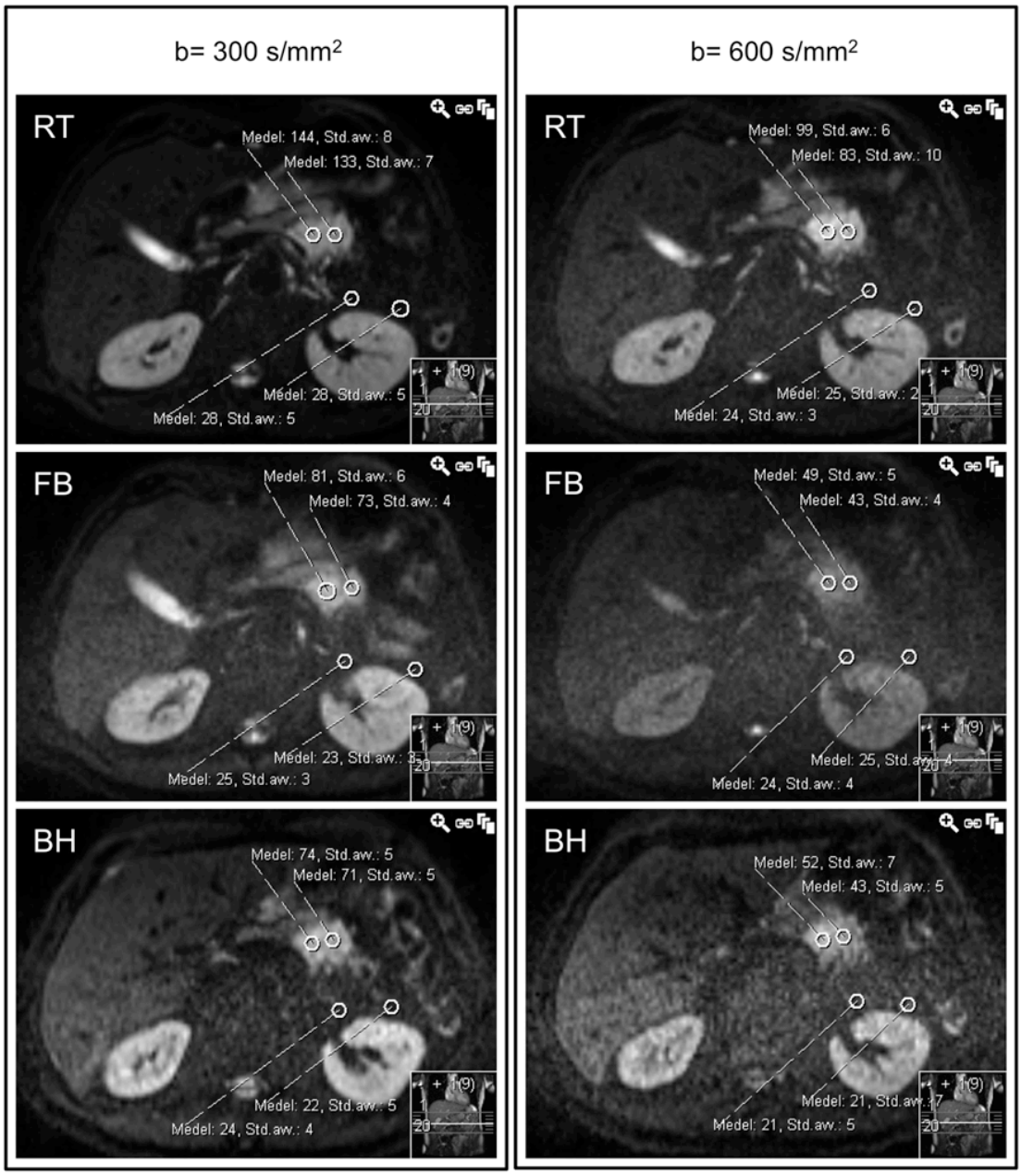

Figure 5. An imaging example of lesion SI as well as noise measurements at the posterior peri-pancreatic space on b300 and b600 for all three techniques. Lesion SI and signal-to-noise ratio (SNR) are clearly higher for RT (upper row) compared to FB (middle row) and BH (lower row)

Table 5. Lesion signal intensity (SI) and signal-to-noise ratio (SNR) for RT, FB and BH techniques and all b-values used

b-value	RT	FB	BH	RT vs. FB	RT vs. BH	FB vs. BH
		Mean SI				
50	154	95	96	*P*<0.05	*P*<0.05	NS
300	106	67	68	*P*<0.05	*P*<0.05	NS
600	75	47	46	*P*<0.05	*P*<0.05	NS
1,000	50	33	30	*P*<0.05	*P*<0.05	NS
		Mean SNR				
50	28	24	18	NS	*P*<0.05	NS
300	27	20	18	*P*<0.05	*P*<0.05	NS
600	21	15	11	*P*<0.05	*P*<0.05	NS
1,000	16	12	8	NS	*P*<0.05	NS

NS = not significant

b) Mean values of ADC_{RT}, ADC_{FB} and ADC_{BH} were 1.20, 1.13 and 1.25 x 10^{-3} mm^2/s respectively. There was no significant difference between RT and BH techniques; BH was significantly higher compared to FB. Mean CVs of ADC_{RT}, ADC_{FB} and ADC_{BH} were 8.9, 10.8 and 14.1 % respectively.
The mean CV of ADC_{RT} was lower –but not significantly– compared to CV of ADC_{FB}. Both were significantly lower than the CV of ADC_{BH} BH (Table 6).

Table 6. Mean ADC values and mean values of coefficient of variation (CV) of ADC for RT, FB and BH techniques

	RT	FB	BH	RT vs. FB	RT vs. BH	FB vs. BH
Mean ADC ($x10^{-3}$ mm/s^2)	1.201	1.132	1.253	NS	NS	*P*<0.05
Mean CV of ADC (%)	8.9	10.8	14.1	NS	*P*<0.05	*P*<0.05

Study III: The study results were as follows:

Lesion detection analysis: At the unenhanced T1-weighted image series, 27 of 44 metastases were detected (sensitivity 61 %, Table 7).

Table 7. The number of liver metastases detected before and after contrast medium administration

	Unenhanced	CMC-001	Gadobenate dimeglumine
True Positive	27[A]	41[B]	42[C]
False Negative	17	3	2
False Positive	7	15	2
Sensitivity	61%	93%	95%

A vs. B $P<0.0001$, A vs. C $P<0.0001$, B vs. C not significant

After contrast medium administration, a statistically significantly greater number of metastases were detected: after CMC-001, 41 of 44 metastases were detected (sensitivity 93 %, $P<0.01$) and after gadobenate dimeglumine 42 of 44 metastases were detected (sensitivity 95 %, $P<0.001$) (Figure 6).

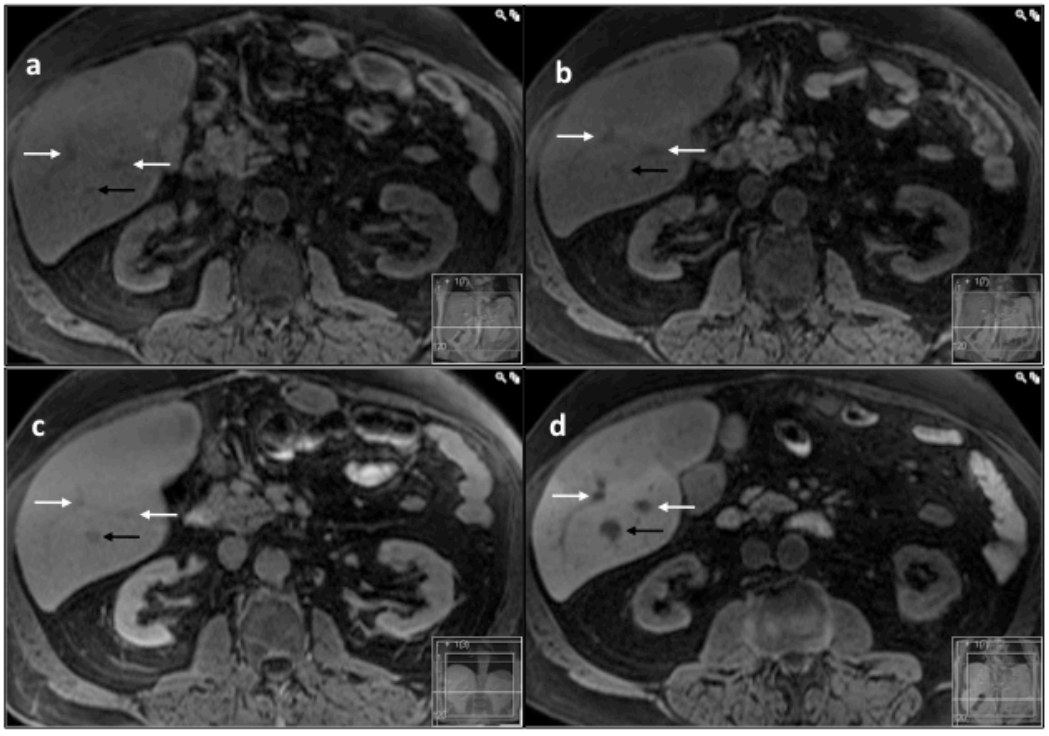

Figure 6. A typical case of colorectal liver metastasis. On the T1-weighted images, the metastasis (black arrow) has lower signal intensity compared to the surrounding liver parenchyma at all phases –before contrast administration (a,b), two hours after intravenous administration of gadobenate dimeglumine (c) and three hours after oral ingestion of CMC-001 (d). Some grade of enhancement of the lesion is observed after intravenous administration of gadobenate dimeglumine (c) but not after ingestion of CMC-001 (d). The white arrows indicate liver vessels.

There was no statistically significant difference in the number of detected metastases between CMC-001 and gadobenate dimeglumine. There were more false positive lesions detected at CMC-001 than at gadobenate dimeglumine (Table 8).

Table 8. False positive lesions

	CMC-001	Gadobenate dimeglumine
FNH	4*	
Haemangioma	4	
Fibrotic haemangioma	2	2
Vessel	2	
Dysfunction / low uptake	2**	
Clips	1	
Total	15	2

*all focal nodular hyperplasias (FNH) were observed in the same patient

** both false positive lesions observed in the same patient

A false positive result for both CMC-001 and gadobenate dimeglumine-enhanced liver MRI is presented in Figure 7.

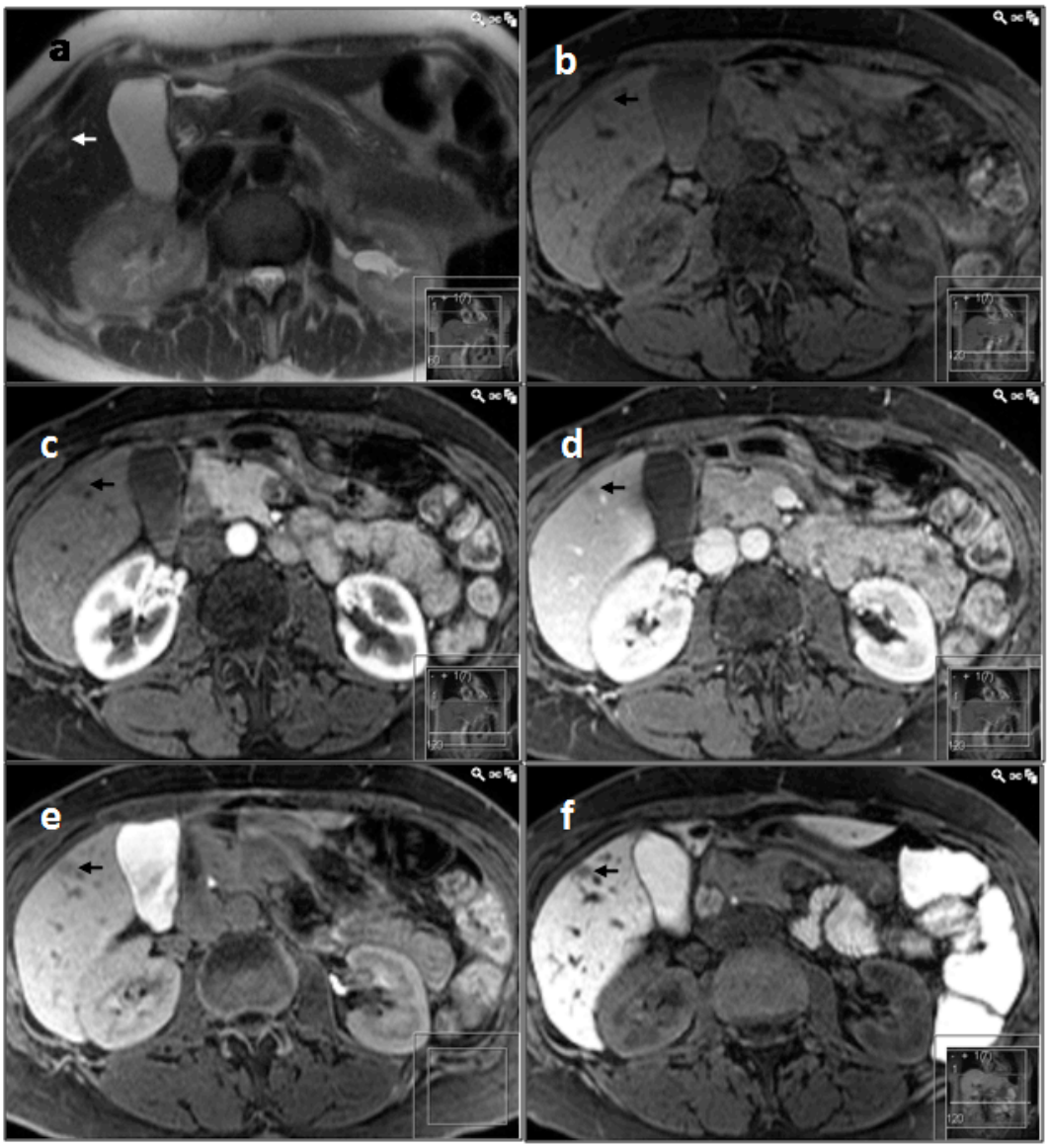

Figure 7. A histopathologically proven fibrotic haemangioma (arrow) being falsely classified as metastasis on both gadobenate dimeglumine and CMC-001 enhanced MRI. On a T2-HASTE image (a), the lesion is faintly hyperintense (arrow). On the T1-weighted images, both before (b) and after injection of gadobenate dimeglumine [arterial (c), portal venous (d) and hepatobiliary (e) phases] as well as 3 hours after ingestion of CMC-001 (f), the lesion has low signal intensity, being impossible to differentiate from metastasis.

Quantitative analysis: The mean metastasis-to-liver ratio increased from 0.22 (SD=0.16) before administration of contrast to 0.51 after CMC-001 (SD=0.17) $P<0.0001$, but was unchanged after gadobenate dimeglumine [0.21 (SD=0.15) before and 0.21 (SD=0.09) after] (Table 9).

Table 9. Mean signal intensity (SI), of liver and metastases before and after contrast medium administration. The SI is in arbitrary units (one standard deviation within parenthesis)

	CMC		Gadobenate dimeglumine	
	Unenhanced	Post contrast 3 hours	Unenhanced	Post contrast 2 hours
Liver SI	160 (35)	268 (91)[A]	160 (37)	267 (75)[B]
Metastasis SI	122 (27)	122 (31)[C]	127 (32)	207 (53)[D]
Metastasis to liver ratio	0.22 (0.16)	0.51 (0.17)[E]	0.21 (0.15)	0.21 (0.09)[F]

A vs. B not significant

C vs. D $P< 0.0001$

E vs. F $P< 0.0001$

Safety analysis: A total of 38 unique AE were reported in 19 patients. After CMC-001 administration, there were 31 AE reported (24 judged to be ADR) and after gadobenate dimeglumine, there were 9 AE reported (3 judged to be ADR). The number of patients with at least 1 AE was 19 after CMC-001 and 8 after gadobenate dimeglumine (Table 10).

Table 10. Total number of participants and occurrence of adverse events (AE) and adverse drug reactions (ADR), and intensity of AE for CMC-001 and gadobenate dimeglumine enhanced liver MRI

	CMC-001	Gadobenate dimeglumine
Total number of participants	20	20
Participants with at least one AE	19 (95%)	8 (40%)
Number of ADR/AE	24/31	3/9
Intensity of AE (mild/moderate/severe)	20/10/1	7/2/0

The most common AE were diarrhoea (12 AE in total, 12 after CMC-001 and 0 after gadobenate dimeglumine) and nausea (4 after CMC-001 and 2 after gadobenate dimeglumine). The most common ADR was diarrhoea (12 after CMC-001 and 0 after gadobenate dimeglumine) followed by supraventricular extrasystoles (1 after CMC-001 and 0 after gadobenate dimeglumine), back pain (1 after CMC-001 and 0 after gadobenate dimeglumine), headache (1 after CMC-001 and 0 after gadobenate dimeglumine) and urticaria (0 after CMC-001 and 1 after gadobenate dimeglumine).
The majority of adverse events were mild (20 AE after CMC-001 and 7 after gadobenate dimeglumine) or moderate (10 AE after CMC-001 and 2 after gadobenate dimeglumine). One AE (back pain judged to be possibly related to CMC-001) was recorded as severe in intensity. No serious AE were reported.
There were no clinically significant changes in clinical laboratory changes, vital signs, ECG or at physical examination.

Study IV: The study results were as follows:

Primary efficacy variable: The increase in liver-to-muscle SI ratio from baseline to post-contrast was most pronounced at the 0.8 g dose level (mean increase in ratio=0.696; SD=0.238), followed by the 0.4 g dose level (0.458; 0.272) and 0.2 g dose level (0.223; 0.143) (Figure 8); there was statistical significance (P<0.0001) in all three pairwise comparisons (Table 11).

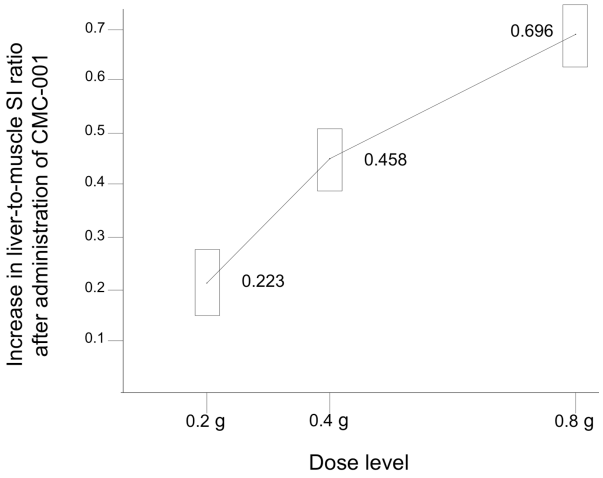

Figure 8. The increase in liver-to-muscle signal intensity (SI) ratio after administration of CMC-001 versus each dose level. Points indicate mean values and bars 95% confidence intervals.

Table 11. Mean increase in liver-to-muscle SI ratio and relative increase in liver SI from baseline to post-contrast for each dose level of the contrast agent CMC-001

	0.8 g	0.4 g	0.2 g
Increase in liver-to-muscle SI ratio (SD)	0.696 (0.238)[a]	0.458 (0.272)[b]	0.223 (0.143)[c]
Relative increase in liver SI, in %	57[d]	33[e]	19[f]

a vs. b P<0.0001, a vs. c P<0.0001, b vs. c P<0.0001
d vs. e P<0.05, d vs. f P<0.05, e vs. f P<0.05
SD: standard deviation

Secondary efficacy variables:
i) Relative increase in liver SI from baseline to post-contrast: The mean relative increase in liver SI was higher for the 0.8 g dose level (57 %) compared to the 0.4 g dose level (33 %) and the 0.2 g dose level (19 %). There was statistical significance (P<0.05) in all three pairwise comparisons (Table 11).

ii) Ranking of overall image quality of post-contrast images: The most frequent ranking at the 0.8 g dose level was superior (17 of 30 MR images); at the 0.4 g dose level it was intermediate (16 of 30 MR images); and at the 0.2 g dose level it was inferior (19 of 30), with all pairwise comparisons between the three dose levels having statistically significant difference (P<0.05) (Table 12 and Figure 9).

Table 12. Ranking of overall image quality* for each dose level of the contrast agent CMC-001

	0.8 g	0.4 g	0.2 g
Superior	17	7	6
Intermediate	9	16	5
Inferior	4	7	19

*For details please see Materials and Methods section
0.8g vs. 0.4g P<0.05; 0.8g vs. 0.2g P<0.001; 0.4g vs. 0.2g P<0.01

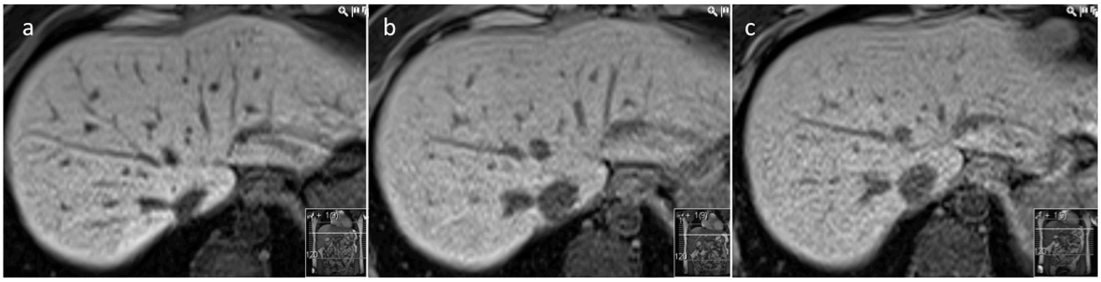

Figure 9. Fat-saturated 3D gradient-echo T1-weighted images of a healthy male volunteer 3 hours after oral ingestion of 0.8 g (a), 0.4 g (b) and 0.2 g (c) of the contrast agent CMC-001 on three different occasions. With regard to overall image quality, image (a) was ranked superior, image (b) intermediate, and image (c) inferior. The three different image sets were viewed simultaneously. Each image was optimized using the F1 function of the workstation (for details, please see Materials and Methods section).

iii) Overall contrast medium uptake in the liver: 93% of participants (28 of 30) showed better results in overall contrast medium uptake in the liver at the 0.8 g and 57% (17 of 30) at the 0.4 g dose levels compared to the 0.2 g dose level (P<0.001 and P>0.05, respectively). At the 0.8 g dose level, 70% of participants (21 of 30) showed better results compared to the 0.4 g dose level (P<0.01) (Figure 10).

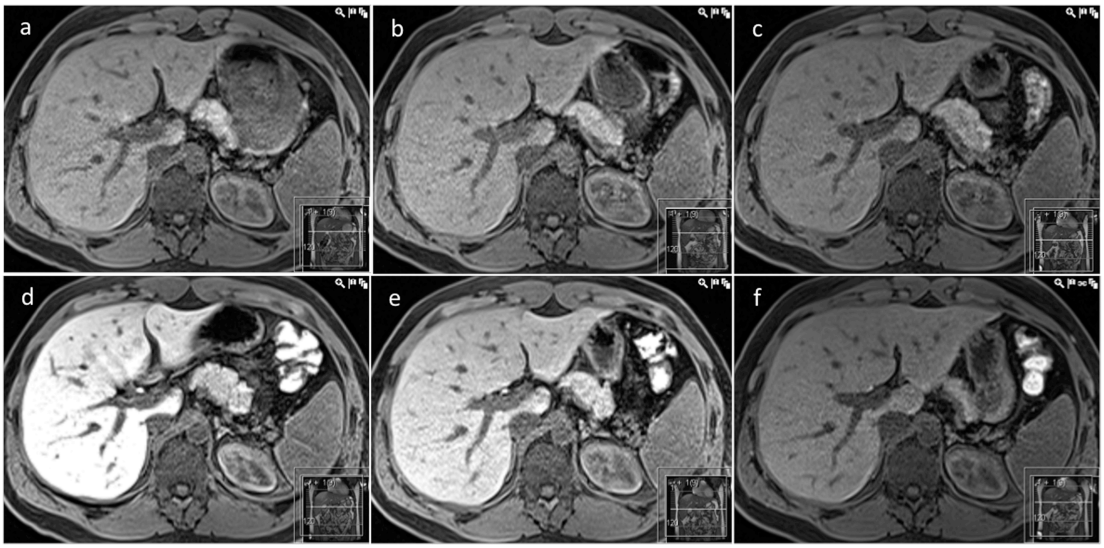

Figure 10. Fat-saturated 3D gradient-echo T1-weighted images of the same volunteer as in Figure 9. Images before (a) and after (d) ingestion of 0.8 g, before (b) and after (e) ingestion of 0.4 g, and before (c) and after (f) ingestion of 0.2 g. The overall contrast medium uptake was rated as excellent in (d), good in (e), and poor in (f). Images after contrast (d,e,f) were viewed simultaneously with the respective unenhanced images (a,b,c). The window level/center settings were optimized using the parameters of the unenhanced images (for details, please see Materials and Methods section).

iv) Homogeneity of contrast medium uptake in the liver: Irrespective of dose level, most participants had the same results for homogeneity of contrast medium uptake in the liver.

Safety:
i) Adverse events: A total of 89 AEs were reported in the study (Table 13).

Table 13. Overview of adverse events (AE) and adverse drug reactions (ADR) for each dose level of the contrast agent CMC-001

	0.8 g	0.4 g	0.2 g
Total number of participants	31[a]	31[a]	30
Participants with at least one AE	25 (80.6%)	18 (58.1%)	10 (33.3%)
Participants with at least one ADR	22 (71.0 %)	13 (41.9 %)	7 (23.3%)
Number of unique[b] ADRs/AEs	37/44	15/27	8/15

[a] data obtained from individuals that were exposed to at least one dose level of CMC-001; for details please see Materials and Methods section

[b] i.e. those ADRs/AEs of a specific preferred term, counted only once in each participant and dose level

The most common AEs were gastrointestinal disorders (diarrhoea, 19; nausea, 19; flatulence, 9), followed by nervous system disorders (headache, 9). Sixty-two of these 89 were considered to be ADRs. The number of participants with at least one ADR increased with increasing dose level. Likewise, the number of unique ADRs increased with increasing dose level (Table 13). All cases of diarrhoea, all but two cases of nausea, all cases of flatulence and 2 of the 9 reported cases of headache were considered to be ADRs (Table 14).

Table 14. The most common adverse drug reactions (ADRs) for each dose level of the contrast agent CMC-001

	ADR	0.8 g	0.4 g	0.2 g
Gastrointestinal disorders	Total	32	11	8
	Diarrhoea	12	2	5
	Nausea	13	2	2
	Flatulence	6	3	0
Nervous system disorders	Total	1	1	0
	Headache	1	1	0
General disorders	Total	2	1	0
	Fatigue	2	1	0

Of the 89 AEs reported in the study only two were considered to be severe in intensity (Table 15). These were two cases of diarrhoea (1 at the 0.8 g dose level and 1 at the 0.2 g dose level), and both were considered ADRs. Eight were considered ADRs with moderate intensity (diarrhoea 3; nausea 2; flatulence 2; vomiting 1). There were no serious ADRs leading to discontinuation of the investigational product.

Table 15. Number of serious, severe, moderate and mild ADRs/AEs for each dose level of the contrast agent CMC-001

	0.8 g	0.4 g	0.2 g
Serious ADRs/AEs	0/0	0/0	0/0
Severe ADRs/AEs	1/1	0/0	1/1
Moderate ADRs/AEs	6/8	1/4	1/1
Mild ADRs/AEs	32/37	14/24	6/13

ii) Physical examination: No clinically significant abnormalities were recorded in the study.
iii) Vital signs (blood pressure, heart rate): No clinically significant abnormalities were recorded in the study.
iv) Electrocardiogram (ECG): No clinically significant abnormalities were recorded in the study.
v) Clinical laboratory evaluation (standard safety parameters): Occasional out-of-range values were observed for the clinical chemistry, haematology and urinalysis parameters assessed in the study. Of these, some were considered to be possibly related to the administration of CMC-001: white blood cell elevation of mild intensity was observed after receiving the 0.4 g dose level (2 participants) and the 0.8 g dose level (2 participants).
vi) Manganese blood concentration: There were no out-of-range values for manganese blood concentration. However, an increase of mean manganese blood concentration was observed with increasing dose levels. Specifically, at the 0.8 g dose level, 165 (SD=44) nmol/L was observed before and 193 (48) nmol/L 3 hours after ingestion, while at the 0.4 g dose level, 173 (42) nmol/L was observed before and 185 (47) nmol/L 3 hours after, and at the 0.2 g dose level, 170 (43) nmol/L was observed before and 179 (46) nmol/L 3 hours after.

5 DISCUSSION

Studies I and II:

The results from **study I** showed that qualitative DWI of pancreatic cancer had an accuracy of 96 % that is similar to the comprehensive MRI protocol in that study population. Besides, the sensitivity and specificity of 92 % and 97 % are comparable to corresponding data (96.2 % and 98.6 %) in a study on DWI by Ichikawa et al. (25). Dynamic gadolinium-enhanced MRI without DWI has been reported having sensitivity and specificity up to 97.7 % and 85.1 %, respectively (53). Multidetector CT (MDCT), positron emission tomography with computed tomography (PET-CT), endoscopic ultrasound (EUS) have a reported sensitivity of 94 %, 89 % and 100 %, respectively and specificity of 87 %, 88 % and 50 %, respectively (54-56). Transabdominal ultrasound has been reported having sensitivity and specificity of up to 86 and 88 %, respectively, if a clinical diagnosis was permitted. However, if including patients where the gland was obscured, on the grounds of body habitus or interposition of gas-filled bowel loops, the sensitivity drops to 63 % (57). In the population of study I (*n*=75), 11 out of 12 patients with malignant tumours were correctly diagnosed using DWI and in only two patients there were false positive lesions. Additionally, the mean ADC values of malignant tumours were significantly lower compared to benign lesions but, as mentioned earlier, there was a considerable overlap as four of the benign lesions had ADC values in the range of malignant lesions. This indicates that qualitative DWI seems to be more accurate than the quantitative analysis and can be used as an accurate method for detection of pancreatic cancer. If positive, a complementary comprehensive study (MRI or MDCT) will probably be needed for staging. If negative, then pancreatic cancer is excluded (NPV of 98 %) and the forthcoming investigations can be more focused on other entities presenting with similar symptoms. From our experience, both the examination and the reading time are much shorter for DWI compared to comprehensive MRI, which further speaks in favour of DWI.

One of the false positive DWI lesions in study I was a pseudocyst with restricted diffusion. To our knowledge, there is no previous study pointing out that pseudocysts can show some grade of restriction in diffusion. However, abscesses in the brain show restricted diffusion and is thought to be due to its content of high-viscosity fluid with necrotic and inflammatory cells (58,59). Thus, the restricted diffusion in the false positive pseudocyst could be due to high-viscosity inflammatory content. The patient did not at the time of examination show any clinical signs of abscess. The other false positive lesion was a small lymph node very near the dorsal aspect of the uncinate process, which had high signal appearance on DW images and low signal on ADC maps, and was misinterpreted as a malignant lesion within the pancreatic gland. The T2-HASTE sequence could not help in correct characterization of the lesion because of its inherent difficulties in depicting lymph nodes. The observation that lymph nodes can have a high signal intensity on DW images and low signal in ADC maps –and thus mislead– is in agreement with other authors (60,61). The false negative DWI lesion was an adenocarcinoma in a patient that had received down-staging radio-/chemotherapy and did not exhibit high signal on DW images; this finding may represent good

response to treatment, in accordance with previously reported results supporting that DWI can be useful in monitoring treatment effects for various malignancies, as shown for both primary (29,30,62,63) and secondary hepatic cancers (28,64-66). However, two other patients with adenocarcinoma that had also been treated with radio- and/or chemotherapy showed positive findings for malignancy on DWI. Both these patients with positive findings on DWI showed tumour progress at follow up and passed away 15 and 18 months after the MRI examination, respectively. On the contrary, the patient with a negative DWI was still alive at latest available follow up (20 months after the MR examination). This may indicate that the former two patients were poor responders and that DWI can help in the evaluation of response to treatment. However, studies dedicated to clarify whether DWI can be used to evaluate response after various therapies in pancreatic malignancies are needed. Furthermore, DWI correctly characterized a mass-forming pancreatitis in two patients that was falsely characterised as a malignant lesion on MRI-c. The finding that these inflammatory pseudotumours did not show high signal intensity on DW images is in accordance with the work of Takeuchi et al. (60). A third patient with mass-forming pancreatitis was correctly characterised with both methods. Whether DWI can help in distinguishing mass-forming pancreatitis from malignancy, which is a common problem in every day clinical practice, has to be examined in studies with larger patient groups. Recently published data in the literature indicate that this differentiation is probably not possible because mass-forming pancreatitis can show both higher and lower ADC values compared with adenocarcinoma, as both entities have a variable grade of fibrosis leading to restriction of free diffusion of water molecules (67-69). However, there is increasing evidence that intravoxel incoherent motion-derived (IVIM) parameters may help in the distinction of these two entities and can be of clinical value (70).

The choice of b-values in the application of DWI in the upper abdomen is a compromise. Low b-values leads to contamination of other forms of intravoxel incoherent motion such as perfusion in the capillary bed, which results in increased ADC values (71,72). At high b-values a decrease in SNR is seen and long acquisition times are required. As a compromise a b-value of 500 s/mm² was chosen. It has more recently been reported that higher b-values, such as 1,000 s/mm², have high sensitivity and specificity for malignant abdominal tumours (73) and in the detection of pancreatic adenocarcinoma (25,60,74). The results presented here, using a b-value of 500 s/mm², had a sensitivity and specificity of 92 and 97 % respectively, in diagnosing pancreatic cancer. The number of averages (NEX) is also important. Increasing the number of averages gives higher SNR but causes prolonged acquisition time. In the present study, we had relatively few NEX and in many patients the anatomical resolution was insufficient and had to be combined with a T2-weighted sequence for detailed anatomical mapping, which has also been proposed by Tsushima et al. (73). With the use of more averages the T2-HASTE sequence for anatomical mapping might be redundant. One possible explanation for the higher sensitivity of DWI in the study of Ichikawa et al. can be the use of higher b-values and/or more NEX compared to the present study.

In populations at high risk for pancreatic cancer, e.g. in individuals with two or more first-grade relatives suffering from pancreatic cancer, and those with known hereditary pancreatic cancer syndromes (hereditary pancreatitis, Peutz-Jegher's syndrome, familial

breast cancer syndromes), a cost-effective screening method is needed. According to a cost-effectiveness study by Rulyak et al. (75), on individuals with pancreatic dysplasia in familial pancreatic cancer kindreds, it is cost-effective to use EUS if the sensitivity is higher than 84 % in a study group with a prevalence of the disease of 16 % or more. In the present study, the sensitivity and the prevalence were on these levels. Therefore, if the cost of a pancreatic DWI does not exceed that of an EUS, the former might also be cost-effective in screening for pancreatic malignancy. Besides, DWI is non-invasive in contrast to EUS and by not employing ionizing radiation it is an appealing cross-sectional imaging alternative to MDCT for screening these patients –especially the younger ones– avoiding multiple radiation exposures. At our institution, we have already implemented DWI plus T2-HASTE for investigating patients for whom contrast-enhanced CT or MR studies are contraindicated, namely those with prior allergic reaction to contrast agents or those with impaired renal function.

Limitations of our study include the relatively small number of cases with malignancy and the retrospective analysis. However, the study material was collected in a prospective and consecutive manner, which reduces the impact of the latter limitation. Finally, a possible limitation is that the image evaluation was performed in consensus from the two participating radiologists. The disadvantages of this approach are the risk of investigator bias and the risk that the results might be worse in a clinical setting (depending on the radiologist's skill); however, the advantage of this approach is that the influence of the radiologist's skill and of random error is reduced, giving the best possible outcome. Besides, it corresponds to the clinical daily routine with primary and secondary readings, which regularly results in a consensus.

In **study II**, the results of the qualitative analysis showed that the total image quality score of the respiratory-triggered technique was significantly higher compared to free-breathing and higher, though not significantly, compared to the breath-hold technique. In the literature, there are no relevant studies comparing these three techniques on DWI of pancreatic ductal adenocarcinoma. In a study by Taouli et al. comparing respiratory-triggered and breath-hold techniques in patients with liver lesions (76), respiratory-triggering showed significantly better subjective image quality, which is in line with our results. However, our results did not completely concur with those of Taouli et al. in that, in our study, respiratory-triggered had better but not significantly better subjective image quality compared to breath-hold. As shown in Table 3, respiratory-triggered had higher score for the anatomy parameter compared to both free-breathing and breath-hold, resulting most probably from a combination of higher SNR and diminished data mis-registration. Even in the ranking of the techniques, respiratory-triggered was ranked significantly higher than both free-breathing and breath-hold by each reader separately as well as on average.

In the quantitative analysis, the mean SI of lesions on all b-values was significantly higher on respiratory-triggered technique compared to free-breathing and breath-hold. Likewise, mean SNRs of lesions were higher on respiratory-triggered technique compared to free-breathing and breath-hold, reaching statistical significance on b-values of 300 and 600 s/mm², which is the b-value interval most commonly used and recommended (77), indicating the clear superiority of respiratory-triggered technique.

SNR for the breath-hold technique was lower for all b-values compared to respiratory-triggered and free-breathing, reaching statistical significance only for the former.
Mean ADC values of lesions on respiratory-triggered and breath-hold did not differ significantly; breath-hold was significantly higher than free-breathing. In the studies by Taouli et al. and Kim et al. (76,78), mean ADC values of liver lesions were significantly higher for respiratory-triggered technique compared to breath-hold, a finding that does not completely concur with our results. A possible explanation could be the different technique used in their studies, namely that all breath-hold DWI images were obtained at a single breath-hold. In our study II, we obtained DWI images for a given b-value at separate breath-holds, where a slight variation at end inspiration may influence the calculation of ADC values. Additional factors that could account for this discrepancy might include differences in tumour characteristics as well as technical aspects related to the MR systems.
The mean coefficient of variation (CV) of the ADC of lesions was lower but not significantly lower for respiratory-triggered technique compared to free-breathing. Both were significantly lower than that of breath-hold technique, making ADC calculations obtained on respiratory-triggered the more precise ones. Taouli et al. also found that for both liver lesions and liver parenchyma, the mean CV of ADC values on respiratory-triggered technique was significantly lower compared to breath-hold (76).

Our study has several limitations. Firstly, the study design included the acquisition of more b-values than recommended and commonly used (77). This had a major implication for the acquisition of images using the breath-hold technique. In practice, this approach does not allow image acquisition at a single breath-hold, eliminating the major advantages of the breath-hold approach, i.e. the shorter acquisition time. Our purpose was, however, to evaluate and compare these three different techniques in a manner as precise and equivalent as possible, focussing on qualitative and quantitative factors. An additional limitation is the fact that for the quantitative evaluation, the number of ROIs placed at the lesion and in fat in the posterior peri-pancreatic space was not always constant: it varied between two and three, potentially leading to calculation errors. However, this was performed consecutively with all three techniques and with all patients, thus minimising this risk. Furthermore, a factor that has to be kept in mind is that our study was performed to the MRI system of one particular vendor and our results may not readily apply to MRI systems from other vendors. Finally, the study population was rather small. However, the results showing which technique performed best, correlated well in both analyses, making us believe that these results are valid nonetheless.

Studies III and IV:

In **study III**, it was shown that the sensitivity to detect CRLM after orally administered manganese (93 %) was comparable to that of intravenously administered gadobenate dimeglumine (95 %). The high level of sensitivity concur with previously published studies on detection of liver metastases at MRI using intravenously administered mangafodipir trisodium (79) and gadobenate dimeglumine (80,81). Additionally, it was found that small CRLM, as small as 3 mm, could be detected both with manganese and gadobenate dimeglumine. The novel contrast agent CMC-001 has, therefore, the potential to be used for surveillance of patients at high risk of liver metastases, distinguishing those cancer patients who need more extensive liver evaluation from those who do not. Such a group of patients is those with colorectal cancer, who require surveillance as well as post-treatment follow-up imaging for several years, preferentially with a fast and sensitive method. However, it needs to be stressed that the present study was conducted in patients with known and/or highly suspected CRLM, which may lead to overestimation of the absolute values of sensitivity for detecting liver metastases; further studies assessing the effectiveness of CMC-001 enhanced liver MRI, as a surveillance tool and follow-up imaging modality after surgery, are warranted.

An advantage of CMC-001 is that it allows patients to self-administer the contrast agent orally 2-3 hours before the imaging acquisition session and, thus, obviating the need for intravenous injection. Furthermore, both the examination and reading times are much shorter for CMC-001 compared to gadobenate dimeglumine; for example acquisition time for CMC-001 is about 10 minutes while for the comprehensive gadobenate dimeglumine about 60+10 minutes. It is however arguable, whether only the delayed imaging series (e.g. late phase after the intravenous administration gadobenate dimeglumine or gadoxetic acid) could be used to reduce both the examination and reading times. To our knowledge, such an approach has not been used, probably because of the costs associated with the supervision needed after intravenous contrast administration and the reluctance to deliberately refrain from obtaining information from the dynamic contrast-enhanced series that could have been accessible.

A high false positive rate is a downside of CMC-001. There were 15 false positive lesions at the CMC-001 session compared with 2 false positive results at the gadobenate dimeglumine. The latter gives additional information about the contrast behaviour of lesions, at the dynamic phases after contrast injection, resulting in higher specificity. In clinical practice, this means that when lesions are detected at CMC-001 enhanced liver MRI, further evaluation by more specific techniques is necessary. Once these lesions have been characterized, CMC-001 enhanced liver MRI should be highly accurate for detecting new lesions. CMC-001 should therefore be of special value in patients where repeated MRI examinations are needed, i.e. in the surveillance situation as well as at follow-up examinations after various treatment options. In the study setting, the radiologists were not allowed to evaluate previous examinations or patient history. This is a limitation of the study, leading to an overestimation of the number of false positive lesions.

When comparing the signal intensity of the liver parenchyma, there was no difference in the signal increase after CMC-001 compared with that after gadobenate dimeglumine (Table 9). However, the metastases did also show some grade of enhancement after gadobenate dimeglumine, but not after CMC-001. Thus, there was a significant increase in the metastasis-to-liver ratio after CMC-001, but not after gadobenate dimeglumine. This finding –i.e. no significant increase in metastasis-to-liver ratio after administration of gadobenate dimeglumine– coupled with the fact that there was a significantly higher metastases detection rate after gadobenate dimeglumine compared to that of the unenhanced series, may appear somehow puzzling. Our explanation for this is as follows: the calculated metastasis-to-liver SI ratio was based on the average SI obtained from region of interest (ROI) placed in metastasis and liver. During the hepatobiliary (or, 2 hour-) phase after the administration of gadobenate dimeglumine, there is still some enhancement of the liver vessels (82). This increases the average SI of the metastases, resulting in unchanged metastasis-to-liver SI ratio; however, it also results in the metastases having a spotted appearance, enabling their distinction from the surrounding liver parenchyma.

In study III, the sensitivity to detect CRLM on T1-weighted images without contrast media was low (61 %), which is much lower compared with previously published data by Choi et al. (81) with sensitivity of 86 % before and 96 % after gadobenate dimeglumine. One possible explanation for their greater sensitivity before contrast media were administered can be the fact that the readers in Choi's study also had access to T2-weighted images, while in our study, readers evaluated only T1-weighted images at the unenhanced session. Interestingly, their sensitivity increased only to 87 % when adding the dynamic phases after gadobenate dimeglumine injection (excluding the hepatobiliary phase), and the number of false positive lesions increased from 0 to 1. Furthermore, published data from Kim et al. (80) show that the hepatobiliary (one-hour delayed) phase had a better diagnostic performance than the dynamic phases imaging after gadobenate dimeglumine injection for the detection of liver metastases (sensitivity of 96 % and 77 %, respectively). These findings indicate that the hepatobiliary phase can play an important role in the evaluation of CRLM.

The dominant excretion of manganese via the hepatobiliary pathway makes it theoretically attractive for use in patients with impaired renal function. When measuring manganese levels in blood levels and urine in healthy volunteers after ingestion of CMC-001, no significant increase in manganese concentration was detected (83). Further safety studies are, however, needed before such recommendations can be issued.

There were no serious AE. All but one of the AE were considered to be of mild or moderate intensity and no safety concerns were raised for any of the to contrast agents. The observed AE after the administration of 1.6 g of CMC-001 were related to the high ion-content resulting in gastrointestinal discomfort, diarrhoea and nausea. Although not serious, AE after CMC-001 were numerous and clearly of higher frequency than those reported by others, being a factor that could potentially inhibit a widespread use (83-86). Therefore we initiated the investigation presented in study IV, with the aim to investigate whether lowering the dose of $MnCl_2$ tetrahydrate could result in fewer AE but with a sufficient diagnostic imaging quality. Apart from the gastrointestinal

disorders, a limitation of using CMC-001 can be the inhomogeneous uptake in cases of low portal venous perfusion and/or of decreased liver function increasing the risk for suboptimal enhancement and diminishing lesion conspicuity.

In study III, all patients were evaluated for liver surgery. Therefore, a majority of the metastases (25/44) could be verified at histopathology. However, the remaining 19 lesions were not considered resectable and therefore they lack histopathological verification. The final diagnosis of these had to rely on other imaging studies and on follow-up. This is a limitation of our study and a factor for potential bias and overestimation of sensitivity. Additionally, our patient cohort, i.e. those with colorectal cancer and high risk of having liver metastases, comprise a highly selected study population, potentially also contributing to an overestimation of sensitivity. However, these limitations are considered to be of low impact in the present comparison with the comprehensive gadobenate dimeglumine protocol. An additional possible limitation –in similarity to study I– is that the image evaluation was performed in consensus between the two participating radiologists. The disadvantages of this approach, as addressed earlier, are the risk of investigator bias and the risk that the results might be worse in a clinical setting, where every radiologist is at his/her own. However, the advantage of this approach is that the influence of the radiologist's skill and of random error is reduced, giving the best possible outcome. Moreover, it corresponds to the clinical daily routine with primary and secondary readings, which regularly results in a consensus.

In **study IV**, it was shown that the efficacy of the 0.8 g dose level of hepatobiliary contrast agent CMC-001 is higher than the dose level of 0.4 g and 0.2 g. The differences were statistically significant, with the highest increase in liver-to-muscle SI ratio seen after administration of the 0.8 g dose level. This increase in SI of the liver parenchyma made it easier to delineate small vessels in the periphery of the liver at the 0.8 g dose level compared to 0.4 g and 0.2 g, resulting in a higher ranking of the 0.8 g dose level images with regard to the overall image quality. The appearance of colorectal cancer liver metastases resembles that of dark vessels, as shown in study III. Thus, one can assume that if small peripheral vessels are clearly defined, then even metastases of similarly small size could be detected and delineated. The 0.8 g dose level, with its significantly better efficacy, is therefore preferred with regard to image quality.
Regarding the safety results (the secondary objective of study IV), no safety concerns were identified in terms of reported ADRs and AEs, clinically relevant abnormalities or trends in physical examination, vital signs, ECG, laboratory values or manganese blood concentration. There was, however, an increase of manganese blood concentration with increasing dose levels. This indicates that small amounts of manganese do reach the systemic circulation. However, the blood levels of manganese did not exceed the reference values. Furthermore, there were differences in the frequency of reported ADRs/AEs between the three different dose levels assessed, where a greater number of ADRs/AEs were observed with increasing dose level. The most common AE was diarrhoea, followed by nausea, flatulence, and headache. Of the 89 AEs reported in the study, 74 were considered mild, 13 moderate and 2 severe in intensity. The 2 AEs reported as severe were cases of diarrhoea (0.8 and 0.2 g dose levels). The participant

with severe diarrhoea after administration of 0.8 g reported diarrhoea of mild intensity before the CMC-001 administration; thus, the diarrhoea worsened after CMC-001 administration. The participant with severe diarrhoea after 0.2 g had no diarrhoea after administration of the higher dose levels. As shown in study III, side effects following administration of 1.6 g of CMC-001 occurred in 19 out of 20 patients (95 %); in study IV, side effects following the administration of a 0.8 g dose occurred in 25 of 31 patients (81 %). None of the ADRs led to discontinuation of the investigational product, and none required hospitalization or medication, with the exception of mild analgesics for headache. Thus, the lowest dose, i.e. 0.2 g, has the lowest frequency and intensity of occurring ADRs/AEs. However, the 0.8 g dose level of CMC-001 is relatively well tolerated.

The reason for not including the 1.6 g dose level was the relatively high frequency of gastrointestinal side effects we had previously encountered in study III. Interestingly, in a recent study by Rief et al., the authors could not observe any statistically significant difference in liver signal intensity enhancement or liver-to-lesion contrast between the 0.8 g and 1.6 g dose levels in patients with liver metastases from various primary malignancies (49). The results of Rief et al. contradict those from a previously published study by Chabanova et al., where it was shown that the 1.6 g dose level caused a more pronounced increase in SI of liver compared to the 0.8 g dose level (86). The study by Chabanova had, however, a clearly different study design. As Rief et al. pointed out, the results of their study were preliminary and should be further validated in a larger number of subjects. It was, anyhow, an indication that the 0.8 g dose level may suffice in the clinical setting, justifying our choice not to include the 1.6 g dose level in the current evaluation.

One limitation of study IV is that the study population was comprised of healthy young volunteers, as opposed to the intended target patient group, namely patients with CRLM. Data available from our study III, show that there is no uptake of CMC-001 contrast agent in metastases, muscle or liver vessels. This allows the use of muscle as an internal reference and liver vessels as a substitute for CRLM when evaluating the liver of healthy volunteers, which indicates that our results can be applicable to patients with CRLM. One possible further limitation is that a safety analysis separately for each promoter for bowel wall absorption, i.e. alanine and vitamin D_3, was not performed. However, there are no data in the literature suggesting that these two promoters –in the amounts used for the three doses of CMC-001 tested in the current study– would pose any safety concerns. Namely, alanine is included in the FDA's list of nutrients and dietary supplements that are generally recognized as safe (87) and for vitamin D_3, the lowest observed adverse effect level (LOAEL) is 3800 IU per day being well above 800 IU, which was the highest level used in the current study (88).

6 CONCLUSIONS

In conclusion of **study I**, DWI –in combination with T2-HASTE– had an accuracy similar to a comprehensive MRI examination for the detection of pancreatic cancer. In cases of positive findings for malignancy, a comprehensive MRI or MDCT examination is probably needed for further characterisation and staging.

In conclusion of **study II**, the respiratory-triggered technique showed superior subjective image quality as well as better signal intensity (SI) characteristics and ADC measurements, and would therefore seem to be the optimal technique for DWI of pancreatic ductal adenocarcinoma.

In conclusion of **study III**, the sensitivity to detect liver metastases from colorectal cancer was, at CMC-001-enhanced MRI, comparably high to that of a comprehensive intravenous gadobenate dimeglumine protocol; and its use was safe, without serious adverse events.

In conclusion of **study IV**, the 0.8 g dose level of the orally administered manganese-based contrast agent CMC-001 provided clearly higher SI enhancement and better imaging quality compared to the 0.4 g and 0.2 g dose levels, thus rendering the 0.8 g dose level the most efficacious of the three. This is at the expense of more frequent ADRs/AEs, which are, however, predominantly of mild intensity and should be endurable for the intended patient group. The use of CMC-001 raised no safety concerns and the use of the 0.8 g dose level is recommended ahead of those of 0.4 g and 0.2 g.

7 FUTURE ASPECTS

Future aspects regarding DWI and the investigation of pancreatic cancer (studies I and II): For lesion detection and characterization in cases of patients with pancreatic cancer, the role of DW imaging is well documented (67). However, standardization of the DWI protocol is lacking. Guidelines suggesting how many and which b-values that should be used, in both everyday clinical practice as well as in the research setting, are needed. In our group, we are currently evaluating –in patients with proven pancreatic cancer that have prospectively undergone free-breathing DWI with 8 b-values (0, 50, 100, 150, 200, 300, 600, 1,000 s/mm²)– if there is a difference in image quality and ADC calculations between multiple, different combinations of b-values. Furthermore, it is of particular interest to investigate whether DWI can be used as a reliable screening tool for pancreatic cancer (89). In a recently published study where DWI was used in combination with transabdominal ultrasound (90), the authors concluded that DWI can be useful in screening for pancreatic cancer. However, large-scale trials are warranted.
Another area of great interest, in the application of DWI (including intravoxel incoherent motion-derived parameters) in patients with pancreatic malignancies, is whether it can predict response to chemo- and/or radiation therapy, and whether it can monitor treatment response. Currently in the literature, there is only one study on the use of apparent diffusion coefficient for predicting response to chemotherapy in patients with advanced pancreatic cancer (91). The authors concluded that lower pre-treatment ADCs on high b-value ADC maps (b=1,000 s/mm²) were predictive of earlier progression. This finding is somehow contradictive to both preclinical and clinical studies where tumours with higher ADC values respond less favourably to various treatments (92). Thus, the value of DWI in pre-treatment prediction of therapy effectiveness in pancreatic cancer has to be further investigated.

Future aspects regarding the orally administered manganese-based contrast agent CMC-001 and the investigation of patients with suspected and/or known colorectal cancer liver metastases (studies III and IV): As pointed out previously, the role of CMC-001 enhanced liver MRI as a surveillance tool in the case of CRLM has to be proven in larger, dedicated prospective studies. Furthermore, of particular interest in this setting is the evaluation of the role of DWI of the liver in combination with the orally administered CMC-001 in order to increase specificity. In a study by Koh et al. (93), the authors showed that by adding DWI to the intravenously administered, manganese-based, liver-specific contrast agent mangafodipir trisodium they could improve the diagnostic accuracy for the detection of CRLM compared with that of either technique alone. DWI was particularly helpful in cases of metastases of small size (<1 cm) or those close to the edge of the liver. In an analogous manner, it is reasonable to believe that by adding DWI to CMC-001-enhanced MRI, the low specificity of the latter could substantially improve, strengthening its role as a potential surveillance tool. Moreover, the combined use of orally administered CMC-001 and intravenously administered extracellular gadolinium may further increase sensitivity and specificity. Finally, it would be of interest to evaluate the role of CMC-001 in detecting hepatocellular carcinoma (HCC) in patients with or without cirrhosis as well as its role in assessing liver function.

8 ACKNOWLEDGEMENTS

All studies were carried out at the Division of Medical Imaging and Technology, Department of Clinical Science, Intervention and Technology (CLINTEC) at Karolinska Institutet, Stockholm and the Department of Radiology, Karolinska University Hospital, Huddinge.

I would like to sincerely thank all who contributed for completing this thesis.

I especially want to thank my principal supervisor associate professor **Nils Albiin** for his outstanding engagement, enthusiasm, support and excellent guidance through all these studies, in research and in general. I consider myself particularly lucky to have worked with such a colleague, researcher and friend!

I also want to express my gratitude to:

My co-supervisor professor **Peter Aspelin** for believing in me and for providing an excellent scientific environment for this thesis to be carried out. His great experience and immediate support, when needed, made any difficulties seem trivial!

My co-supervisor associate professor **Torkel Brismar** for sharing his knowledge, ideas and optimism as well as for always helping, when needed.

My co-supervisor professor **Johan Permert** for enriching this thesis with his ideas and invaluable comments in many occasions.

My surgeon colleagues and co-authors **Ralf Segersvärd** and **Christian Kylander** for including patients and their co-authoring contributions.

My co-authors **Terri Lindholm**, **Louiza Loizou**, **Annika Bergqvist** and **Bita Sadigh** for their multiple contributions. Especially, I would like to express my sincere sympathy to the family of my beloved colleague and co-author **Nick Edsborg**, who is no longer with us. We will all miss a dear friend and colleague.

The present and former head of the Department of Radiology at Karolinska University Hospital, Huddinge **Maria Kristoffersen-Wiberg**, **Henry Lindholm** and **Bo Persson** for supporting my efforts and providing the time and resources needed for completing this thesis.

My colleagues **Eva Gröndahl** and **Elisabet Axelsson** for planning the clinical schedule in such a way that my research project could proceed unhampered as well as all my colleagues, especially in the abdominal section, for their friendliness and continuous support.

Our secretaries **Helena Forssell** och **Maj-Britt Stäring** for their invaluable help and friendliness during all these years.

All MRI-technologists and physicists at Karolinska University Hospital, Huddinge for their excellent examinations, friendliness and patience both with our patients and ourselves. Furthermore, all personnel at the Department of Radiology, Karolinska University Hospital, Huddinge for contributing with one way or the other.

The friends and shareholders of the CMC Contrast AB (Lyngby, Denmart) **Jan Trøst Jørgensen** och **Thomas Grönberg** for allowing me to participate in studies III and IV and use them as a substantial part of this thesis.

Our statistician and friend **Per Näsman** for the excellent and time-efficient co-operation.

The director of studies at the Doctoral School for Clinicians in Epidemiology (generation 7), at Karolinska Institutet, docent Ylva Trolle Lagerros for her enthusiasm and engagement in making our studies an experience at its own.

My mentor and good friend associate professor **Ioannis Dimitriou** for all the good advice and long discussions, independently of time during the day.

Finally, I would like to express a huge thanks to my mother **Sofia**, who alongside my father **Georgios** during his life, provided an invaluable guidance, supported me at all my steps and embraced me with their love. Last but not least, I thank my partner **Kyriaki** for her unconditional love and support during all our common years.

9 REFERENCES

1. McSweeney SE, O'Donoghue PM, Jhaveri K. Current and emerging techniques in gastrointestinal imaging. J Postgrad Med. 2010 Apr-Jun;56(2):109-16. Review. PubMed PMID: 20622390.
2. Hyslop WB, Balci NC, Semelka RC. Future horizons in MR imaging. Magn Reson Imaging Clin N Am. 2005 May;13(2):211-24. Review. PubMed PMID: 15935308.
3. Pauwels EK, Bourguignon M. Cancer induction caused by radiation due to computed tomography: a critical note. Acta Radiol. 2011 Sep 1;52(7):767-73. Epub 2011 Jul 8. Review. PubMed PMID: 21742785
4. Jemal A, Siegel R, Ward E, Hao Y, Xu J, Murray T, Thun MJ. Cancer statistics, 2008. CA Cancer J Clin. 2008 Mar-Apr;58(2):71-96.Epub 2008 Feb 20. PubMed PMID: 18287387.
5. Ferlay J, Shin HR, Bray F, Forman D, Mathers C, Parkin DM. Estimates of worldwide burden of cancer in 2008: GLOBOCAN 2008. Int J Cancer. 2010 Dec 15;127(12):2893-917. PubMed PMID: 21351269.
6. Li D, Xie K, Wolff R, Abbruzzese JL. Pancreatic cancer. Lancet. 2004 Mar 27;363(9414):1049-57. Review. PubMed PMID: 15051286.
7. Le Bihan D, Breton E, Lallemand D, Grenier P, Cabanis E, Laval-Jeantet M. MR imaging of intravoxel incoherent motions: application to diffusion and perfusion in neurologic disorders. Radiology. 1986 Nov;161(2):401-7. PubMed PMID: 3763909.
8. Robertson RL, Glasier CM. Diffusion-weighted imaging of the brain in infants and children. Pediatr Radiol. 2007 Aug;37(8):749-68. Epub 2007 Jun 23. Review. PubMed PMID: 17589837.
9. Eustace S, DiMasi M, Adams J, Ward R, Caruthers S, McAlindon T. In vitro and in vivo spin echo diffusion imaging characteristics of synovial fluid: potential non-invasive differentiation of inflammatory and degenerative arthritis. Skeletal Radiol. 2000 Jun;29(6):320-3. PubMed PMID: 10929413.
10. Nonomura Y, Yasumoto M, Yoshimura R, Haraguchi K, Ito S, Akashi T, Ohashi I. Relationship between bone marrow cellularity and apparent diffusion coefficient. J Magn Reson Imaging. 2001 May;13(5):757-60. PubMed PMID: 11329198.
11. Morgan VA, Kyriazi S, Ashley SE, DeSouza NM. Evaluation of the potential of diffusion-weighted imaging in prostate cancer detection. Acta Radiol. 2007 Jul;48(6):695-703. PubMed PMID: 17611881.
12. Matsuki M, Inada Y, Tatsugami F, Tanikake M, Narabayashi I, Katsuoka Y. Diffusion-weighted MR imaging for urinary bladder carcinoma: initial results. Eur Radiol. 2007 Jan;17(1):201-4. Epub 2006 Jul 25. PubMed PMID: 16865369.
13. Tamai K, Koyama T, Saga T, Morisawa N, Fujimoto K, Mikami Y, Togashi K. The utility of diffusion-weighted MR imaging for differentiating uterine sarcomas from benign leiomyomas. Eur Radiol. 2008 Apr;18(4):723-30. Epub 2007 Oct 10. PubMed PMID: 17929022.

14. Ichikawa T, Erturk SM, Motosugi U, Sou H, Iino H, Araki T, Fujii H. High-B-value diffusion-weighted MRI in colorectal cancer. AJR Am J Roentgenol. 2006 Jul;187(1):181-4. PubMed PMID: 16794174.
15. Taouli B, Chouli M, Martin AJ, Qayyum A, Coakley FV, Vilgrain V. Chronic hepatitis: role of diffusion-weighted imaging and diffusion tensor imaging for the diagnosis of liver fibrosis and inflammation. J Magn Reson Imaging. 2008 Jul;28(1):89-95. PubMed PMID: 18581382.
16. Sandrasegaran K, Akisik FM, Lin C, Tahir B, Rajan J, Saxena R, Aisen AM. Value of diffusion-weighted MRI for assessing liver fibrosis and cirrhosis. AJR Am J Roentgenol. 2009 Dec;193(6):1556-60. PubMed PMID: 19933647.
17. Do RK, Chandarana H, Felker E, Hajdu CH, Babb JS, Kim D, Taouli B. Diagnosis of liver fibrosis and cirrhosis with diffusion-weighted imaging: value of normalized apparent diffusion coefficient using the spleen as reference organ. AJR Am J Roentgenol. 2010 Sep;195(3):671-6. Erratum in: AJR Am J Roentgenol. 2010 Oct;195(4):1043. PubMed PMID: 20729445.
18. Lewin M, Poujol-Robert A, Boëlle PY, Wendum D, Lasnier E, Viallon M, Guéchot J, Hoeffel C, Arrivé L, Tubiana JM, Poupon R. Diffusion-weighted magnetic resonance imaging for the assessment of fibrosis in chronic hepatitis C. Hepatology. 2007 Sep;46(3):658-65. PubMed PMID: 17663420.
19. Akisik MF, Aisen AM, Sandrasegaran K, Jennings SG, Lin C, Sherman S, Lin JA, Rydberg M. Assessment of chronic pancreatitis: utility of diffusion-weighted MR imaging with secretin enhancement. Radiology. 2009 Jan;250(1):103-9. Epub 2008 Nov 10. PubMed PMID: 19001148.
20. Erturk SM, Ichikawa T, Motosugi U, Sou H, Araki T. Diffusion-weighted MR imaging in the evaluation of pancreatic exocrine function before and after secretin stimulation. Am J Gastroenterol. 2006 Jan;101(1):133-6. PubMed PMID: 16405545.
21. Kamisawa T, Takuma K, Anjiki H, Egawa N, Hata T, Kurata M, Honda G, Tsuruta K, Suzuki M, Kamata N, Sasaki T. Differentiation of autoimmune pancreatitis from pancreatic cancer by diffusion-weighted MRI. Am J Gastroenterol. 2010 Aug;105(8):1870-5. Epub 2010 Mar 9. PubMed PMID: 20216538.
22. Bruegel M, Holzapfel K, Gaa J, Woertler K, Waldt S, Kiefer B, Stemmer A, Ganter C, Rummeny EJ. Characterization of focal liver lesions by ADC measurements using a respiratory triggered diffusion-weighted single-shot echo-planar MR imaging technique. Eur Radiol. 2008 Mar;18(3):477-85. Epub 2007 Oct 25. PubMed PMID: 17960390.
23. Taouli B, Vilgrain V, Dumont E, Daire JL, Fan B, Menu Y. Evaluation of liver diffusion isotropy and characterization of focal hepatic lesions with two single-shot echo-planar MR imaging sequences: prospective study in 66 patients. Radiology. 2003 Jan;226(1):71-8. PubMed PMID: 12511671.
24. Bakir B, Salmaslioğlu A, Poyanli A, Rozanes I, Acunas B. Diffusion weighted MR imaging of pancreatic islet cell tumors. Eur J Radiol. 2010 Apr;74(1):214-20. Epub 2009 Mar 4. PubMed PMID: 19264435.
25. Ichikawa T, Erturk SM, Motosugi U, Sou H, Iino H, Araki T, Fujii H. High-b value diffusion-weighted MRI for detecting pancreatic adenocarcinoma: preliminary results. AJR Am J Roentgenol. 2007 Feb;188(2):409-14. PubMed PMID: 17242249.

26. Kartalis N, Lindholm TL, Aspelin P, Permert J, Albiin N. Diffusion-weighted magnetic resonance imaging of pancreas tumours. Eur Radiol. 2009 Aug;19(8):1981-90. Epub 2009 Mar 24. PubMed PMID: 19308414.
27. Koh DM, Scurr E, Collins D, Kanber B, Norman A, Leach MO, Husband JE. Predicting response of colorectal hepatic metastasis: value of pretreatment apparent diffusion coefficients. AJR Am J Roentgenol. 2007 Apr;188(4):1001-8. PubMed PMID: 17377036.
28. Cui Y, Zhang XP, Sun YS, Tang L, Shen L. Apparent diffusion coefficient: potential imaging biomarker for prediction and early detection of response to chemotherapy in hepatic metastases. Radiology. 2008 Sep;248(3):894-900. PubMed PMID: 18710982.
29. Mannelli L, Kim S, Hajdu CH, Babb JS, Clark TW, Taouli B. Assessment of tumor necrosis of hepatocellular carcinoma after chemoembolization: diffusion-weighted and contrast-enhanced MRI with histopathologic correlation of the explanted liver. AJR Am J Roentgenol. 2009 Oct;193(4):1044-52. PubMed PMID: 19770328.
30. Kamel IR, Liapi E, Reyes DK, Zahurak M, Bluemke DA, Geschwind JF. Unresectable hepatocellular carcinoma: serial early vascular and cellular changes after transarterial chemoembolization as detected with MR imaging. Radiology. 2009 Feb;250(2):466-73. PubMed PMID: 19188315.
31. Taouli B, Koh DM. Diffusion-weighted MR imaging of the liver. Radiology. 2010 Jan;254(1):47-66. Review. PubMed PMID: 20032142.
32. Manfredi S, Lepage C, Hatem C, Coatmeur O, Faivre J, Bouvier AM. Epidemiology and management of liver metastases from colorectal cancer. Ann Surg. 2006 Aug;244(2):254-9. PubMed PMID: 16858188; PubMed Central PMCID: PMC1602156.
33. Bengmark S, Hafström L. The natural history of primary and secondary malignant tumors of the liver. I. The prognosis for patients with hepatic metastases from colonic and rectal carcinoma by laparotomy. Cancer. 1969 Jan;23(1):198-202. PubMed PMID: 5763253.
34. Abdalla EK, Adam R, Bilchik AJ, Jaeck D, Vauthey JN, Mahvi D. Improving resectability of hepatic colorectal metastases: expert consensus statement. Ann Surg Oncol. 2006 Oct;13(10):1271-80. Epub 2006 Sep 6. PubMed PMID: 16955381.
35. Stangl R, Altendorf-Hofmann A, Charnley RM, Scheele J. Factors influencing the natural history of colorectal liver metastases. Lancet. 1994 Jun 4;343(8910):1405-10. PubMed PMID: 7515134.
36. Giacchetti S, Itzhaki M, Gruia G, Adam R, Zidani R, Kunstlinger F, Brienza S, Alafaci E, Bertheault-Cvitkovic F, Jasmin C, Reynes M, Bismuth H, Misset JL, Lévi F. Long-term survival of patients with unresectable colorectal cancer liver metastases following infusional chemotherapy with 5-fluorouracil, leucovorin, oxaliplatin and surgery. Ann Oncol. 1999 Jun;10(6):663-9. PubMed PMID: 10442188.
37. Choti MA, Sitzmann JV, Tiburi MF, Sumetchotimetha W, Rangsin R, Schulick RD, Lillemoe KD, Yeo CJ, Cameron JL. Trends in long-term survival following liver resection for hepatic colorectal metastases. Ann Surg. 2002 Jun;235(6):759-66. PubMed PMID: 12035031; PubMed Central PMCID: PMC1422504.

38. Zorzi D, Mullen JT, Abdalla EK, Pawlik TM, Andres A, Muratore A, Curley SA, Mentha G, Capussotti L, Vauthey JN. Comparison between hepatic wedge resection and anatomic resection for colorectal liver metastases. J Gastrointest Surg. 2006 Jan;10(1):86-94. PubMed PMID: 16368496.
39. de Jong MC, Pulitano C, Ribero D, Strub J, Mentha G, Schulick RD, Choti MA, Aldrighetti L, Capussotti L, Pawlik TM. Rates and patterns of recurrence following curative intent surgery for colorectal liver metastasis: an international multi-institutional analysis of 1669 patients. Ann Surg. 2009 Sep;250(3):440-8. PubMed PMID: 19730175.
40. The Royal College Of Radiologists Guidelines Working Party. Making the best use of clinical radiology services: a new approach to referral guidelines. Clin Radiol. 2007 Oct;62(10):919-20. Epub 2007 Aug 20. PubMed PMID: 17765455.
41. Schima W, Kulinna C, Langenberger H, Ba-Ssalamah A. Liver metastases of colorectal cancer: US, CT or MR? Cancer Imaging. 2005 Nov 23;5 Spec No A:S149-56. Review. PubMed PMID: 16361131; PubMed Central PMCID: PMC1665297.
42. American College of Radiology (2008) ACR appropriateness criteria: suspected liver metastases. Available via http://www.acr.org/SecondaryMainMenuCategories/quality_safety/app_criteria/pdf/ExpertPanelonGastrointestinalImaging/SuspectedLiverMetastasesDoc14.aspx. Accessed 13 Oct 2010
43. Konopke R, Bunk A, Kersting S. The role of contrast-enhanced ultrasound for focal liver lesion detection: an overview. Ultrasound Med Biol. 2007 Oct;33(10):1515-26. Epub 2007 Jul 6. Review. PubMed PMID: 17618038.
44. Niekel MC, Bipat S, Stoker J. Diagnostic imaging of colorectal liver metastases with CT, MR imaging, FDG PET, and/or FDG PET/CT: a meta-analysis of prospective studies including patients who have not previously undergone treatment. Radiology. 2010 Dec;257(3):674-84. Epub 2010 Sep 9. PubMed PMID:20829538.
45. Martin DR, Danrad R, Hussain SM. MR imaging of the liver. Radiol Clin North Am. 2005 Sep;43(5):861-86, viii. Review. PubMed PMID: 16098344.
46. Floriani I, Torri V, Rulli E, Garavaglia D, Compagnoni A, Salvolini L, Giovagnoni A. Performance of imaging modalities in diagnosis of liver metastases from colorectal cancer: a systematic review and meta-analysis. J Magn Reson Imaging. 2010 Jan;31(1):19-31. Review. PubMed PMID: 20027569.
47. Thomsen HS. Recent hot topics in contrast media. Eur Radiol. 2011 Mar;21(3):492-5. Epub 2010 Dec 7. Review. PubMed PMID: 21136062.
48. Leander P, Golman K, Månsson S, Höglund P. Orally administered manganese with and without ascorbic acid as a liver-specific contrast agent and bowel marker for magnetic resonance imaging: phase I clinical trial assessing efficacy and safety. Invest Radiol. 2010 Sep;45(9):559-64. PubMed PMID: 20644487.
49. Rief M, Huppertz A, Asbach P, Franiel T, Schwenke C, Hamm B, Taupitz M, Wagner M. Manganese-based oral contrast agent for liver magnetic resonance imaging: evaluation of the time course and dose response of liver signal intensity enhancement. Invest Radiol. 2010 Sep;45(9):565-71. PubMed PMID: 20644484.

50. Bellin MF, Webb JA, Van Der Molen AJ, Thomsen HS, Morcos SK; Members of Contrast Media Safety Committee of European Society of Urogenital Radiology (ESUR). Safety of MR liver specific contrast media. Eur Radiol. 2005 Aug;15(8):1607-14. Epub 2004 Dec 31. Review. PubMed PMID: 15627176.
51. Thomsen HS, Svendsen O, Klastrup S. Increased manganese concentration in the liver after oral intake. Acad Radiol. 2004 Jan;11(1):38-44. PubMed PMID: 14746400.
52. Heverhagen Heverhagen JT. Noise measurement and estimation in MR imaging experiments. Radiology. 2007 Dec;245(3):638-9. PubMed PMID: 18024445.
53. Birchard KR, Semelka RC, Hyslop WB, Brown A, Armao D, Firat Z, Vaidean G. Suspected pancreatic cancer: evaluation by dynamic gadolinium-enhanced 3D gradient-echo MRI. AJR Am J Roentgenol. 2005 Sep;185(3):700-3.PubMed PMID: 16120921.
54. Fletcher JG, Wiersema MJ, Farrell MA, Fidler JL, Burgart LJ, Koyama T, Johnson CD, Stephens DH, Ward EM, Harmsen WS. Pancreatic malignancy: value of arterial, pancreatic, and hepatic phase imaging with multi-detector row CT. Radiology. 2003 Oct;229(1):81-90.PubMed PMID: 14519871.
55. Farma JM, Santillan AA, Melis M, Walters J, Belinc D, Chen DT, Eikman EA, Malafa M. PET/CT fusion scan enhances CT staging in patients with pancreatic neoplasms. Ann Surg Oncol. 2008 Sep;15(9):2465-71. Epub 2008 Jun 13. PubMed PMID: 18551347.
56. Agarwal B, Abu-Hamda E, Molke KL, Correa AM, Ho L. Endoscopic ultrasound-guided fine needle aspiration and multidetector spiral CT in the diagnosis of pancreatic cancer. Am J Gastroenterol. 2004 May;99(5):844-50. PubMed PMID: 15128348.
57. Schick V, Franzius C, Beyna T, Oei ML, Schnekenburger J, Weckesser M, Domschke W, Schober O, Heindel W, Pohle T, Juergens KU. Diagnostic impact of 18F-FDG PET-CT evaluating solid pancreatic lesions versus endosonography, endoscopic retrograde cholangio-pancreatography with intraductal ultrasonography and abdominal ultrasound. Eur J Nucl Med Mol Imaging. 2008 Oct;35(10):1775-85. Epub 2008 May 15. PubMed PMID: 18481063.
58. Noguchi K, Watanabe N, Nagayoshi T, Kanazawa T, Toyoshima S, Shimizu M, Seto H. Role of diffusion-weighted echo-planar MRI in distinguishing between brain brain abscess and tumour: a preliminary report. Neuroradiology. 1999 Mar;41(3):171-4. PubMed PMID: 10206159.
59. Mishra AM, Gupta RK, Saksena S, Prasad KN, Pandey CM, Rathore D, Purwar A, Rathore RK, Husain N, Jha DK, Jaggi RS, Husain M. Biological correlates of diffusivity in brain abscess. Magn Reson Med. 2005 Oct;54(4):878-85. PubMed PMID: 16155895.
60. Takeuchi M, Matsuzaki K, Kubo H, Nishitani H. High-b-value diffusion-weighted magnetic resonance imaging of pancreatic cancer and mass-forming chronic pancreatitis: preliminary results. Acta Radiol. 2008 May;49(4):383-6.PubMed PMID: 18415779.
61. Tsushima Y, Takano A, Taketomi-Takahashi A, Endo K. Body diffusion-weighted MR imaging using high b-value for malignant tumor screening: usefulness and necessity of referring to T2-weighted images and creating fusion images. Acad Radiol. 2007 Jun;14(6):643-50. PubMed PMID: 17502253.

62. Schraml C, Schwenzer NF, Martirosian P, Bitzer M, Lauer U, Claussen CD, Horger M. Diffusion-weighted MRI of advanced hepatocellular carcinoma during sorafenib treatment: initial results. AJR Am J Roentgenol. 2009 Oct;193(4):W301-7. PubMed PMID: 19770299.
63. Eccles CL, Haider EA, Haider MA, Fung S, Lockwood G, Dawson LA. Change in diffusion weighted MRI during liver cancer radiotherapy: preliminary observations. Acta Oncol. 2009;48(7):1034-43. PubMed PMID: 19634060.
64. Buijs M, Vossen JA, Hong K, Georgiades CS, Geschwind JF, Kamel IR. Chemoembolization of hepatic metastases from ocular melanoma: assessment of response with contrast-enhanced and diffusion-weighted MRI. AJR Am J Roentgenol. 2008 Jul;191(1):285-9. PubMed PMID: 18562760.
65. Theilmann RJ, Borders R, Trouard TP, Xia G, Outwater E, Ranger-Moore J, Gillies RJ, Stopeck A. Changes in water mobility measured by diffusion MRI predict response of metastatic breast cancer to chemotherapy. Neoplasia. 2004 Nov-Dec;6(6):831-7. PubMed PMID: 15720810; PubMed Central PMCID: PMC1531687.
66. Liapi E, Geschwind JF, Vossen JA, Buijs M, Georgiades CS, Bluemke DA, Kamel IR. Functional MRI evaluation of tumor response in patients with neuroendocrine hepatic metastasis treated with transcatheter arterial chemoembolization. AJR Am J Roentgenol. 2008 Jan;190(1):67-73. PubMed PMID: 18094295.
67. Wang Y, Miller FH, Chen ZE, Merrick L, Mortele KJ, Hoff FL, Hammond NA, Yaghmai V, Nikolaidis P. Diffusion-weighted MR imaging of solid and cystic lesions of the pancreas. Radiographics. 2011 May-Jun;31(3):E47-64. Review. Erratum in: Radiographics. 2011 Sep-Oct;31(5):1496. Vahid, Yaghmai [corrected to Yaghmai, Vahid]. PubMed PMID: 21721197.
68. Huang WC, Sheng J, Chen SY, Lu JP. Differentiation between pancreatic carcinoma and mass-forming chronic pancreatitis: usefulness of high b value diffusion-weighted imaging. J Dig Dis. 2011 Oct;12(5):401-8. PubMed PMID: 21955434.
69. Wiggermann P, Grützmann R, Weissenböck A, Kamusella P, Dittert DD, Stroszczynski C. Apparent diffusion coefficient measurements of the pancreas, pancreas carcinoma, and mass-forming focal pancreatitis. Acta Radiol. 2012 Mar 1;53(2):135-9. Epub 2012 Jan 19. PubMed PMID: 22262868.
70. Klauss M, Lemke A, Grünberg K, Simon D, Re TJ, Wente MN, Laun FB, Kauczor HU, Delorme S, Grenacher L, Stieltjes B. Intravoxel incoherent motion MRI for the differentiation between mass forming chronic pancreatitis and pancreatic carcinoma. Invest Radiol. 2011 Jan;46(1):57-63. PubMed PMID: 21139505.
71. Yamada I, Aung W, Himeno Y, Nakagawa T, Shibuya H. Diffusion coefficients in abdominal organs and hepatic lesions: evaluation with intravoxel incoherent motion echo-planar MR imaging. Radiology. 1999 Mar;210(3):617-23. PubMed PMID: 10207458.
72. Kim T, Murakami T, Takahashi S, Hori M, Tsuda K, Nakamura H. Diffusion-weighted single-shot echoplanar MR imaging for liver disease. AJR Am J Roentgenol. 1999 Aug;173(2):393-8. PubMed PMID: 10430143.
73. Tsushima Y, Takano A, Taketomi-Takahashi A, Endo K. Body diffusion-weighted MR imaging using high b-value for malignant tumor screening:

usefulness and necessity of referring to T2-weighted images and creating fusion images. Acad Radiol. 2007 Jun;14(6):643-50. PubMed PMID: 17502253.
74. Matsuki M, Inada Y, Nakai G, Tatsugami F, Tanikake M, Narabayashi I, Masuda D, Arisaka Y, Takaori K, Tanigawa N. Diffusion-weighed MR imaging of pancreatic carcinoma. Abdom Imaging. 2007 Jul-Aug;32(4):481-3. PubMed PMID: 17431713.
75. Rulyak SJ, Kimmey MB, Veenstra DL, Brentnall TA. Cost-effectiveness of pancreatic cancer screening in familial pancreatic cancer kindreds. Gastrointest Endosc. 2003 Jan;57(1):23-9. PubMed PMID: 12518126.
76. Taouli B, Sandberg A, Stemmer A, Parikh T, Wong S, Xu J, Lee VS. Diffusion-weighted imaging of the liver: comparison of navigator triggered and breathhold acquisitions. J Magn Reson Imaging. 2009 Sep;30(3):561-8. PubMed PMID: 19711402.
77. Padhani AR, Liu G, Koh DM, Chenevert TL, Thoeny HC, Takahara T, Dzik-Jurasz A, Ross BD, Van Cauteren M, Collins D, Hammoud DA, Rustin GJ, Taouli B, Choyke PL. Diffusion-weighted magnetic resonance imaging as a cancer biomarker: consensus and recommendations. Neoplasia. 2009 Feb;11(2):102-25. PubMed PMID: 19186405.
78. Kim SY, Lee SS, Byun JH, Park SH, Kim JK, Park B, Kim N, Lee MG. Malignant hepatic tumors: short-term reproducibility of apparent diffusion coefficients with breath-hold and respiratory-triggered diffusion-weighted MR imaging. Radiology. 2010 Jun;255(3):815-23. PubMed PMID: 20501719.
79. Bartolozzi C, Donati F, Cioni D, Procacci C, Morana G, Chiesa A, Grazioli L, Cittadini G, Cittadini G, Giovagnoni A, Gandini G, Maass J, Lencioni R. Detection of colorectal liver metastases: a prospective multicenter trial comparing unenhanced MRI, MnDPDP-enhanced MRI, and spiral CT. Eur Radiol. 2004 Jan;14(1):14-20. Epub 2003 Aug 9. PubMed PMID: 14730384.
80. Kim YK, Lee JM, Kim CS, Chung GH, Kim CY, Kim IH. Detection of liver metastases: gadobenate dimeglumine-enhanced three-dimensional dynamic phases and one-hour delayed phase MR imaging versus superparamagnetic iron oxide-enhanced MR imaging. Eur Radiol. 2005 Feb;15(2):220-8. Epub 2004 Dec 29. PubMed PMID: 15624108.
81. Choi JY, Choi JS, Kim MJ, Lim JS, Park MS, Kim JH, Chung YE. Detection of hepatic hypovascular metastases: 3D gradient echo MRI using a hepatobiliary contrast agent. J Magn Reson Imaging. 2010 Mar;31(3):571-8. PubMed PMID: 20187199.
82. Brismar TB, Dahlstrom N, Edsborg N, Persson A, Smedby O, Albiin N. Liver vessel enhancement by Gd-BOPTA and Gd-EOB-DTPA: a comparison in healthy volunteers. Acta Radiol. 2009 Sep;50(7):709-15. PubMed PMID: 19701821.
83. Thomsen HS, Loegager V, Noergaard H, Chabanova E, Moller JM, Sonne J. Oral manganese for liver imaging at three different field strengths. Acad Radiol. 2004 Jun;11(6):630-6. PubMed PMID: 15172365.
84. Chabanova E, Logager V, Moller JM, Dekker H, Barentsz J, Thomsen HS. Imaging liver metastases with a new oral manganese-based contrast agent. Acad Radiol. 2006 Jul;13(7):827-32. PubMed PMID: 16777556.
85. Thomsen HS, Barentsz JO, Burcharth F, Chabanova E, Dekker HM, Moesgaard F, Moller JM, Leth-Espensen P, Logager V, Takahashi S. Initial clinical

experience with oral manganese (CMC-001) for liver MR imaging. Eur Radiol. 2007 Jan;17(1):273-8. Epub 2006 Jun 9. PubMed PMID: 16763790.
86. Chabanova E, Thomsen HS, Løgager V, Moller JM, Brage K, Fogh K, Bovin J, Elmig J. Effect of new manganese contrast agent on tissue intensities in human volunteers: comparison of 0.23, 0.6 and 1.5 T MRI, a part of a phase I trial. MAGMA. 2004 Sep;17(1):28-35. Epub 2004 Jul 16. PubMed PMID: 15258827.
87. US Government Printing Office (2000) Section 582.5118—alanine. title 21—food and drugs. Chapter I—Food and Drug Administration, Department of Health and Human Services. Part 582—substances generally recognized as safe. subpart F—Nutrients and/or dietary supplements 1. http://www.gpo.gov/fdsys/pkg/CFR-2000-title21-vol6/xml/CFR-2000-title21-vol6-sec582-5118.xml. Accessed 01 Feb 2012
88. Hollis BW, Wagner CL. Assessment of dietary vitamin D requirements during pregnancy and lactation. Am J Clin Nutr. 2004 May;79(5):717-26. Review. PubMed PMID: 15113709.
89. Klapman J, Malafa MP. Early detection of pancreatic cancer: why, who, and how to screen. Cancer Control. 2008 Oct;15(4):280-7. Review. PubMed PMID: 18813195.
90. Kuroki-Suzuki S, Kuroki Y, Nasu K, Nagashima C, Machida M, Muramatsu Y, Moriyama N. Pancreatic cancer screening employing noncontrast magnetic resonance imaging combined with ultrasonography. Jpn J Radiol. 2011 May;29(4):265-71. Epub 2011 May 24. PubMed PMID: 21607840.
91. Niwa T, Ueno M, Ohkawa S, Yoshida T, Doiuchi T, Ito K, Inoue T. Advanced pancreatic cancer: the use of the apparent diffusion coefficient to predict response to chemotherapy. Br J Radiol. 2009 Jan;82(973):28-34. PubMed PMID: 19095814.
92. Padhani AR. Diffusion magnetic resonance imaging in cancer patient management. Semin Radiat Oncol. 2011 Apr;21(2):119-40. Review. PubMed PMID: 21356480.
93. Koh DM, Brown G, Riddell AM, Scurr E, Collins DJ, Allen SD, Chau I, Cunningham D, deSouza NM, Leach MO, Husband JE. Detection of colorectal hepatic metastases using MnDPDP MR imaging and diffusion-weighted imaging (DWI) alone and in combination. Eur Radiol. 2008 May;18(5):903-10. Epub 2008 Jan 12. PubMed PMID: 18193234.